Spring 2013

Phase behavior and stimuli response in lyotropic liquid crystalline templated photopolymers

Todd James Thorson
University of Iowa

PHASE BEHAVIOR AND STIMULI RESPONSE IN LYOTROPIC LIQUID CRYSTALLINE TEMPLATED PHOTOPOLYMERS

by

Todd James Thorson

A thesis submitted in partial fulfillment of the requirements for the Master of Science degree in Chemical and Biochemical Engineering in the Graduate College of The University of Iowa

May 2013

Thesis Supervisor: Professor C. Allan Guymon

Graduate College
The University of Iowa
Iowa City, Iowa

CERTIFICATE OF APPROVAL

MASTER'S THESIS

This is to certify that the Master's thesis of

Todd James Thorson

has been approved by the Examining Committee for the thesis requirement for the Master of Science degree in Chemical and Biochemical Engineering at the May 2013 graduation.

Thesis Committee:_____
C. Allan Guymon

_____
Julie Jessop

_____
Gary Aurand

TABLE OF CONTENTS

LIST OF FIGURES

CHAPTER I. INTRODUCTION

Polymeric materials that exhibit enhanced transport and mechanical properties and contain periodic nanoscale structures are of recent interest in a number of applications.[1-4] Of particular significance is the use of these nanostructured materials in desalination membranes, biosensors, actuators, and drug delivery vehicles.[3-5] In contrast to an isotropic, traditional polymer, structured polymers contain some variety of repeatable structure throughout the material. This repeatable structure is responsible for imparting altered properties upon the polymer compared to their isotropic, unordered counterparts. In many applications, a material of great mechanical integrity, while allowing useful rates of transport within the material, is desirable. For instance, a biosensor must be able to withstand conditions within the body that might alter the structure of a weaker, less robust material while being able to act at biological speeds and provide a successful response to a stimulus. Research has revealed many methods for enhancing mechanical and transport properties individually, but an increasing number of technological avenues would benefit greatly from the ability to couple both property classes.

Although structured polymeric materials have been extensively studied over the last few decades, a complete understanding of these materials has not yet been reached. In order to produce repeatable features within a polymer, the idea of using a template has proved to be an increasingly successful route. Templating structure onto a polymer involves the use of an additional material arranged in a desired geometry. The premise for this method is simple: monomer added will adopt a specific geometry, polymerization is initiated, and the geometry is templated onto the resulting polymer. A number of templating materials have been used to transfer a desired structure to a polymer.[6-8] One of the simplest methods employs a two-dimensional silica bead array. This method involves multiple steps in which a monomer is first

added to fill the space around the beads and then thermally polymerized to reveal the template. The beads are then dissolved leaving the template for another monomer addition and subsequent polymerization which results in a 2D monolayer of polymer containing repeating pores on the scale of approximately five micrometers.[9]

Another templating method that has garnered interest in the biological community for the mimicking of a biological process is the use of molecular imprint polymers (MIPs).[10,11] MIPs utilize the concept of the "Lock-and-Key" mechanism of enzyme-substrate interactions to preferentially bind to certain substances that fit the imprinted cavity of the MIP. The substrate or species of interest is introduced to monomer which will form a selective cavity around the substrate. The resultant polymer contains the templated cavity necessary for the retention of the target substrate or those similar to the target. This application has received much attention in membrane technology and chemical sensing where the MIP is able to separate or detect target compounds.[10]

Silica beads and MIPs offer viable methods for templating structure onto polymers; however, these materials are limited to the micron scale or cavity based function. The desire to create structural features on the nano-scale has continued to push templated polymer research forward. Researchers have hypothesized that homogenous nanoporous materials would aid in mechanical integrity while providing necessary channels for molecular transport.[4] To achieve structure at the nanoscale, surfactants have been widely studied. Early work with surfactants utilized vesicle templating to produce nanoparticles with a membrane-like polymer shell. These particles are of particular interest in drug delivery applications as a hydrophobic drug could be loaded within the shell and transported to location of significance within the body.[12,13]

1.1 Lyotropic Liquid Crystal Templating

Related closely to the use of surfactants for vesicle templating to reinforce structure is the use of liquid crystals (LCs) as templates for nanostructured polymers. Liquid crystals are regarded as the fourth state of matter as they exist as a fluid, yet exhibit long-range order.[14] Liquid crystals are divided into two main classes: thermotropic and lyotropic. The main difference between the two classes of LCs is the effect that causes orientational or positional order. Temperature effects direct order in thermotropic liquid crystals (TLCs), while concentration effects direct order in lyotropic liquid crystals (LLCs). Self-assembly of LCs is the structure inducing feature in LC templating. TLC molecules are able to self-assemble into ordered phases without the presence of any other substance. This feature has made them the primary focus in polymer-stabilized liquid crystal (PSLC) systems.[6] In PSLC systems, monomer is added to a TLC assembly and polymerized, and the resultant system consists of polymer adopting the long-range TLC structure and the stabilized TLC molecules. Studies have utilized TLCs, particularly PSLCs, as polymer templates to generate nanostructured polymers.[15-19]

In the other case, LLCs exist as amphiphilic molecules which dictate the key feature of LLCs: their ability to self-assemble into different geometries, or mesophases, when influenced by a solvent in order to keep the hydrophilic and hydrophobic constituents in separate domains. Water acts as the solvent in a majority of systems, and LLCs will self-assemble in water based on the hydrophobic effect, grouping hydrophobic ends of each molecule in the LLC mesophase. Although LLC self-assembly can be affected by temperature and pressure, concentration is the primary governing factor in LLC order. Systems are commonly studied at constant temperature and pressure to take advantage of processability at ambient conditions.[7] By modulation of the LLC concentration, the various LLC mesophases exhibiting long-range orientational

nanostructure can be accessed. An idealized progression of the LLC mesophases is shown in Figure 1.1.

The first instance of hydrophobic constituent shielding occurs at the critical micelle concentration (CMC). This is referred to as the micellar mesophase, yet it does not technically exhibit liquid crystalline order; many substances other than liquid crystals are capable of forming a micellar phase.[20] Once the system transitions to the micellar cubic phase with increased surfactant concentration, liquid crystalline order is achieved. In this phase, micelles exhibit long-range order aligning on a cubic lattice. Increasing concentration further leads to the hexagonal phase which consists of closely packed cylinders positioned on a hexagonal lattice, shielding the hydrophobic portion of the liquid crystal in a pore-like structure while the hydrophilic portion makes up the continuous phase. Next, the bicontinuous cubic phase is observed as the hydrophilic and hydrophobic domains exist co-continuously in a gyroid, sponge-like phase.

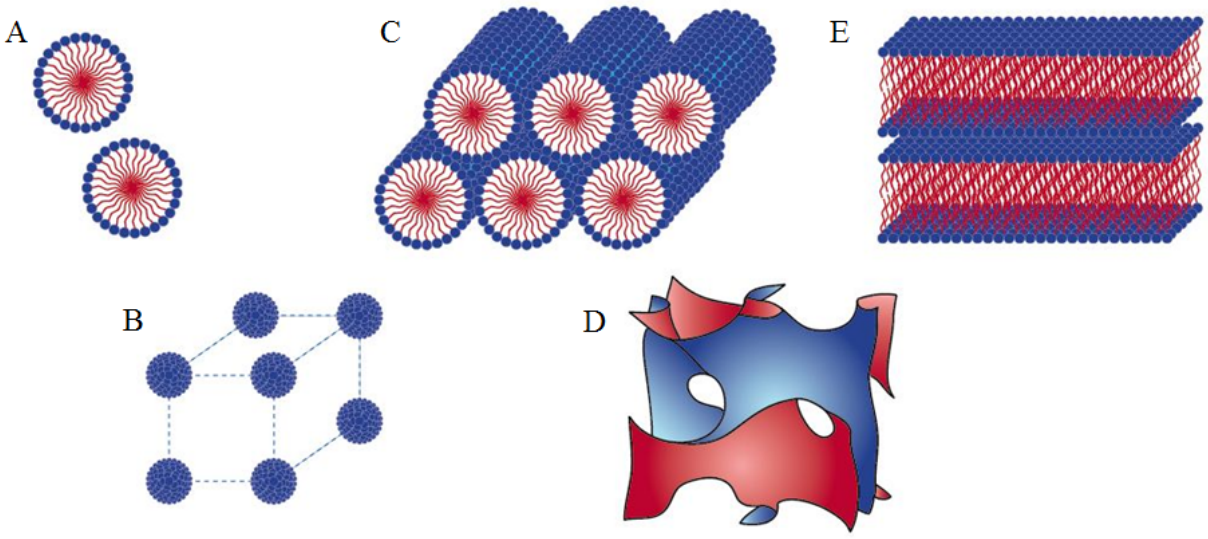

Figure 1.1. Schematic progression of lyotropic liquid crystal mesophases. Shown in order of increasing liquid crystal concentration are the **A**) micellar, **B**) micellar cubic, **C**) hexagonal, **D**) bicontinuous cubic, and **E**) lamellar mesophases.

There are a number of different conformations of the bicontinuous cubic, gyroid phase that assemble along different lattices. The last pictured mesophase existing at high liquid crystal concentration is the lamellar phase. In this phase, liquid crystals self-assemble into bilayers similar to the lipid bilayer of cell membranes. Not pictured, but also studied to a high degree, are inverse phases. These phases exist at very high liquid crystal concentration, and as water becomes scarce in the system, liquid crystals will now self-assemble to shield the small hydrophilic domain. Common inverse mesophases include the inverse hexagonal and inverse micellar phases in which the continuous domains now consist of the hydrophobic LLC chains.[14]

It is important to note that not every LLC system progresses through each of these mesophases. The ability of these molecules to self-assemble in a particular mesophase is dependent upon charge, size, and chemistry of the liquid crystal.[21] Liquid crystals may be ionic or non-ionic, may contain very large or small moieties on their chains, or may have a predominately hydrophilic or hydrophobic nature. The combination of these factors leads to a wide variety of LLC systems, each possessing certain characteristics. Additionally, surfactants themselves can serve as the monomers in LLC systems, which will be discussed in further detail below. Examples of a few surfactants that can form lyotropic liquid crystals are shown in Figure 1.2. Pictured is a non-ionic polyoxyethylene (10) cetyl ether (Brij C10), an anionic sodium dodecyl sulfate (SDS), a cationic cetyl trimethyl ammonium bromide, and a quaternary ammonium surfactant monomer (PM1) containing a reactive group in the nonpolar tail.

This variability in LLCs and their ability to form highly ordered mesophases lend these systems naturally for use as template platforms for generating nanostructured polymers. To use LLC mesophases as templates, monomer is added to the system. Depending on the particular monomer hydrophobicity, added monomer will spontaneously diffuse to the hydrophilic or

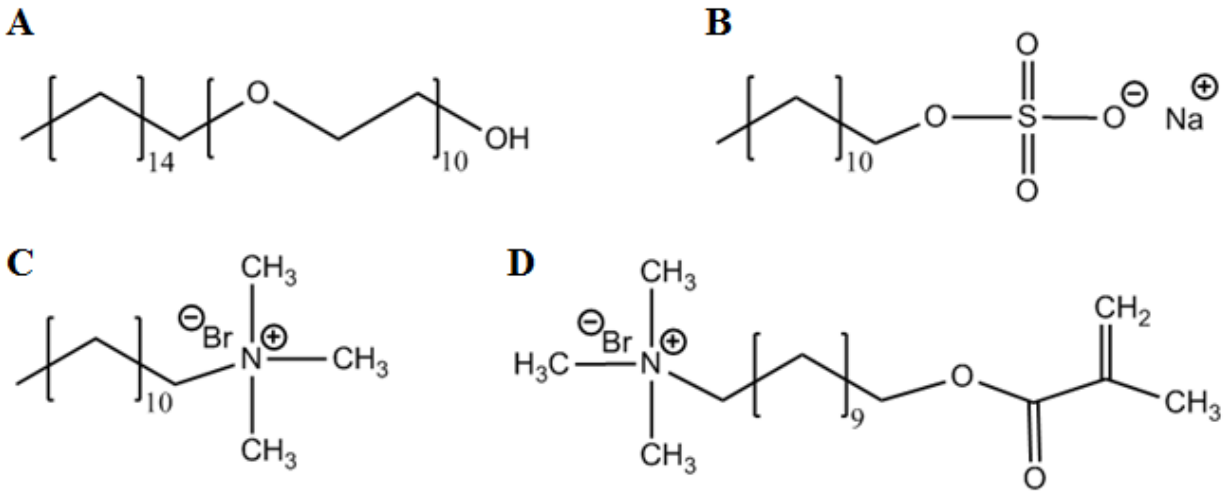

Figure 1.2. Surfactant lyotropic liquid crystal examples. Shown are **A**) Brij C10, **B**) SDS, **C**) DTAB, and **D**) PM1.

hydrophobic domain of the mesophase. From here, the system is polymerized, liquid crystal is removed through solvent-exchange with a solvent such as acetone or ethanol, and the polymer is dried. The final result is a polymer containing the nano-scale features of the parent LLC mesophase template. A schematic of photopolymerization within both domains of the hexagonal LLC template is shown in Figure 1.3.

In an ideal templating process, the final polymer nanostructure exists as a direct, 1-to-1 copy of the mesophase geometry. However, problems have been documented in the direct transfer of the parent template. The largest obstacle to overcome in reaching a high degree of structure retention is unfavorable thermodynamics that evolve throughout polymerization. Many studies using LLCs as templates have discovered phase separation occurring during polymerization resulting in little to no mesophase order in the final polymer. Phase separation is the result of a decrease in entropy of growing polymers confined to the mesophase geometry

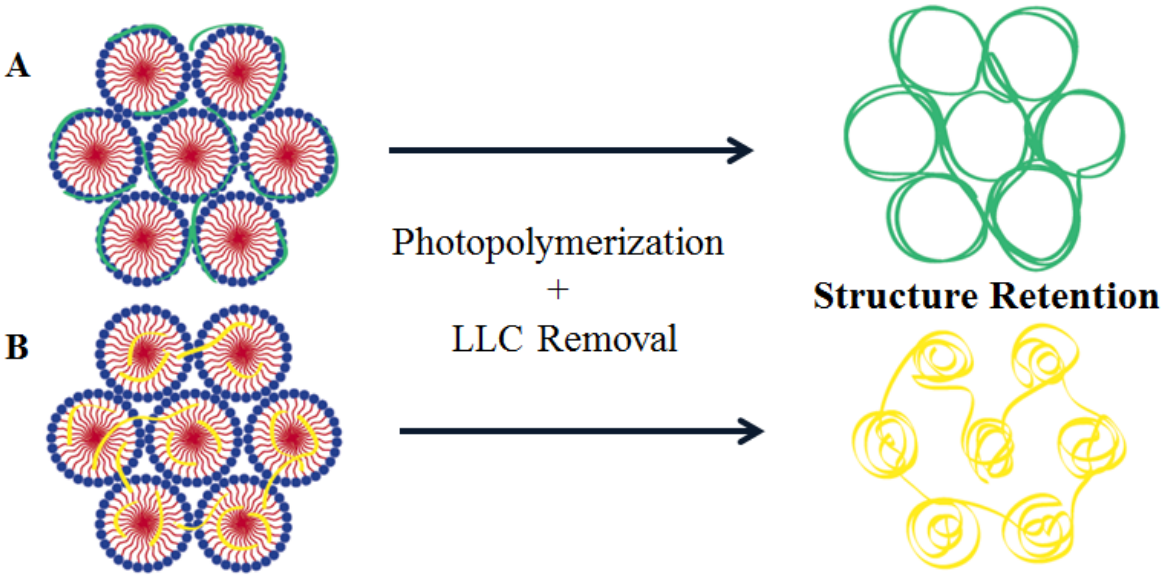

Figure 1.3. Templating process schematic using hexagonal LLC mesophase as template platform in the continuous, hydrophilic domain (**A**) and discontinuous, hydrophobic domain (**B**).

thereby rendering the system thermodynamically unstable. To circumvent phase separation due to thermodynamic instability, photopolymerization has been successfully employed in LLC templated polymers. Photopolymerization initiation rates are inherently rapid; therefore, the speed of the reaction can kinetically trap nanostructure. Photopolymerization offers the additional advantages of spatial and temporal control in that a specific area can be polymerized for any specific time period. The final polymer system resulting in successful photo-initiated templating is still thermodynamically unstable but is now kinetically limited by high polymer viscosity.

Studies of thermally initiated radical polymerizations of various hydrophilic monomers templated by non-ionic surfactants have yielded porous polymer gels; however, the pores in

these materials are several microns indicating phase separation during polymerization.[22] A noteworthy result of this research was the observation that complete loss of order did not take place; this result lends to the idea of partial thermodynamically driven phase separation as the polymerization progresses. Conversely, photo-initiated radical polymerizations in LLC systems have shown great promise in achieving polymers with a high degree of templated liquid crystalline order.[23-25] Poly(ethylene glycol) diacrylate (PEGDA), poly(acrylamide) (PAm), and poly(*N*-isopropylacrylamide) (PNIPAm) are all examples of polymers with great potential that retained high degrees of order when photopolymerized with non-ionic Brij surfactant. PEGDA has received interest in the field of drug delivery due to polymer biocompatibility and release kinetics of model molecules. PAm is already used extensively for protein separation in gel electrophoresis, and interest resides in accessing new separation abilities realized in nanostructured polymers. PNIPAm is the subject of an immense amount of research aimed at controlling and tapping its thermo-responsive behavior for a plethora of applications such as desalination membranes and novel drug delivery vehicles.[3-5,26-28]

Further examination of polymerization kinetics has revealed that increasing the order in the LLC system increases the polymerization rate ten-fold in acrylamide systems templated by non-ionic Brij surfactant. This increase is attributed to decreased diffusion of growing polymer chains and increased local monomer concentration available for polymerization, both influenced by the order of the LLC mesophase. Polymerization rate is also a direct function of the LLC mesophase. In acrylamide systems templated with Brij 58, the polymerization rate maximum increases by a factor of 2.5 when transitioning from a micellar to a bicontinuous cubic phase. The rate maximum then returns to its micellar value as surfactant concentration is increased to access the inverse micellar phase. When the less hydrophilic Brij C10 is used, polymerization

rate increases from micellar to micellar cubic to hexagonal and finally decreases similarly to the Brij 58 system upon the transition to inverse micellar phase. At its peak using a hexagonal templating platform, the acrylamide system exhibits a 10-fold increase in maximum polymerization rate compared to isotropic acrylamide.[29] This kinetic behavior shows the ability to modulate polymerization rates between LLC mesophases in structure retaining acrylamide systems.

Additionally, polymerization kinetics studies in poorly retaining systems have been utilized for analyzing phase separation events. Phase separation is accompanied by a discernible discontinuity in the rate of polymerization.[30] This research has provided insight into phase separation events as a function of reaction conversion. Large morphology variations occurring at low conversions are coupled with a deceleration in polymerization rate, while further loss of structure or morphology variation occurring at intermediate conversion is coupled with rate accelerations. Both studies of photopolymerization kinetics and LLC morphology support the ability to control ultimate nanostructure in templated materials.

Much like the differences observed in photopolymerization kinetics between different LLC mesophases templates, polymer properties are also affected by polymer morphology. The ability to control the porosity, mechanical strength, swelling, and degradation kinetics by a change in LLC concentration provides a simple, low cost route to generate enhanced materials. Many studies have worked at exploiting property changes between LLC templates in a number of different monomer systems.[23,31-35] Photopolymerization of *n*-decyl acrylate within hexagonal and lamellar mesophases revealed an increase in the templated polymer molecular weight, and these changes in molecular weight directly have an effect on polymer properties.[31,36] In one case, water uptake and compressive modulus of PAm and 2-hydroxyethyl methacrylate (HEMA)

templated by various LLC morphologies were examined.[32] Results from this study were contrasting in that considerable increases in both properties were observed in PAm systems while the opposite was observed in HEMA systems when comparing against their traditional, isotropic polymers. These results are important to note because properties can be enhanced or compromised depending on the system and parent template morphology. What is even more important to note is the mechanical behavior observed in PAm systems. Traditionally, polymers swelled with water exhibit decreased mechanical strength, making many materials unsuitable for applications; however, increases in swelling exhibited by PAm are coupled with increases in mechanical strength by as much as three times the isotropic PAm.[33]

Further examination of polymer property modulation has shown the ability to dramatically affect polymer surface area and permeability with templated nanostructure. For instance, both properties in PAm and poly(ethylene glycol) diacrylate (PEGDA) systems are enhanced at least 4-fold in hexagonal, bicontinuous cubic, and lamellar templates.[34] Additionally, dye release behavior and biodegradability have been enhanced using LLC order in poly(ethylene glycol) (PEG) systems.[23,35] Both properties here are influence by the material's ability to accelerate transport of water, dye, and cleaved units due to increased porosity and swelling.

It is evident that further understanding of the thermodynamics of LLC systems before, during, and after polymerization must be gained in order to fully grasp control over LLC templated materials. One possible route for studying the thermodynamic behavior responsible for disrupting liquid crystalline order during polymerization is using model simulations. Linear triblock copolymers have been modeled using Monte Carlo simulations that take into account interaction parameters of each polymer chain.[37,38] Using similar modeling methods is a

promising avenue for modeling LLC behavior as liquid crystals interact and form similar phases as the polymers studied. These copolymers behave similarly to surfactant molecules due to their hydrophobic and hydrophilic blocks. Interaction parameters between molecules in LLC systems that must be considered include dipole-dipole interactions, induction forces, dispersion forces, and London forces between the surfactants.[14] If the model was translated to incorporate the much smaller liquid crystal molecules as well as monomer, new insight could dramatically impact future work in LLC templated polymers.

LLCs not only can be used to create the template platform for nanostructured materials, they can be used to create the template themselves in the case of photopolymerizable surfactants. Photopolymerizable surfactants can be utilized for further templating of additional polymers or act simply as the final polymer material. Researchers have probed the effects of polymerizable functionality location on the surfactant molecule to find that polymerization rates increase or decrease with LLC order when the functionality is either located near the polar group or far from the polar group, respectively.[39] Polymerizable surfactants have also been used to create new materials for catalysis and membrane applications. For instance, cross-linking of the inverse hexagonal phase provides an open pore system that has been used to moderate conversion of inorganic reactants. Additionally, cross-linking of butyl rubber with polymerizable surfactants in this same phase provides a defense against large, hydrophobic chemical warfare molecules while providing breathability through hydro-selective pores. Butyl rubber-surfactant material has also been polymerized in the bicontinuous cubic phase for use as desalination membranes. The selective nature of this material arises simply from the size scale of water molecules and hydrolyzed ions as only water molecules are small enough to diffuse through the nanometer-wide continuous channels.[1,2] Polymerizable surfactants have also found their way into LLC

systems as structure stabilizers in previously poor structure retaining systems.[40] Increasing polymerizable surfactant concentration enhances structure retention in polyacrylamide systems templated with a cationic surfactant that exhibited poor structure retention in the original system.

Further research into the use of polymerizable surfactants as structure stabilizers has revealed changes in polymer properties on top of structure retention. Not only is the equilibrium swelling of materials templated in a hexagonal mesophase increased by approximately 10%, the hydrated compressive modulus remains comparable to isotropic hydrogels and is even increased in dry testing. Furthermore, dye release is facilitated in the hexagonally templated hydrogels based upon increased porosity as previously discussed.[40]

1.2 Stimuli-Sensitive Polymers

Enhanced properties realized in nanostructured polymers have the potential to affect a number of different areas within polymer science and beyond. One gaining much momentum in recent years is their use in the field of stimuli-sensitive polymers. These polymers respond to physical or chemical cues and could provide a promising avenue for developing "smart polymeric gels."[5] Stimuli-sensitive materials are of particular significance in biomaterials applications where a response to an external stimulus could trigger changes in biomolecule adhesion, regulation of ions, or biochemical signal conversion.[41]

Stimuli-sensitive polymers are classified according to the stimulus that causes the desired response. A stimulus can be either physical (e.g. magnetic, light) or chemical (e.g. biological, electrochemical) in nature, but of the many possible stimuli, pH, analyte, and temperature sensitive materials have received considerable attention.[42] Acidic or alkaline functional groups on a polymer are characteristic of pH-sensitive polymers. In these materials, the response is a

change in hydrodynamic volume or swelling behavior due to electrostatic forces with the degree of ionization of the polymer chain dictates the magnitude of the repulsion forces, thus, the degree of polymer swelling.[43] Target pH responsiveness varies considerably depending on the target application. In biological research, the different pH of organs or biological systems lends itself naturally to pH-sensitive polymers. For instance, a material administered orally that is sensitive to a pH value of 5 would undergo a transition as it passed from a digesting stomach of pH 4 to the intestine at pH 5.5. A specific area of research concerning biological pH-sensitive polymers is controlled gene delivery. Currently, the large negative charge of DNA makes it a very difficult molecule to transport; bonding DNA with a cationic pH-sensitive polymer such as poly(L-lysine) (PLL) creates a multi-charged complex capable of transport throughout the body. Theoretically, PLL will respond to the delivery target pH thereby releasing the gene from the complex for therapy.[44,45]

Like pH-sensitive polymers, analyte-sensitive polymers are intriguing materials for physiological applications. The idea of physiologically relevant analyte-sensitive polymers is based highly on feedback regulation within the body. Feedback regulation is responsible for a multitude of processes such as blood sugar regulation in which insulin is released only when high blood sugar levels are detected. Examples of analyte-sensitive polymer research receiving attention include glucose-sensitive, glutathione-sensitive, antigen-sensitive, and metabolite-sensitive polymers. In the aforementioned blood sugar regulation, glucose-sensitive polymers provide a promising route for improved insulin drug delivery. Interestingly, pH-sensitivity can be coupled with glucose sensitivity in controlling drug release. For instance, poly(acrylic acid) (PAA) conjugated with the glucose-sensitive enzyme glucose oxidase (GOx) in microcapsules loaded with insulin have been prepared.[46,47] Upon glucose binding as a substrate to GOx,

gluconic acid is released, initiating a volume transition in PAA due to a decrease in pH value and subsequent release of insulin to the blood. Other interesting analyte-sensitive materials incorporate a previously discussed templating method, molecular imprint polymers (MIPs).[48] As discussed, response in MIPs is triggered by recognition of the imprint or mimic molecule.

The third example and topic of the research performed in Chapter 5 is temperature-sensitive or thermo-sensitive polymers. Thermo-responsiveness in polymers is by no means a new discovery; response to temperature exhibited by poly(acrylamide) (PAm) was first observed in 1978.[49] Since then, much attention has been given to thermo-sensitive materials for biomaterials and many other applications. Block copolymers of various compositions of poly(ethylene oxide) (PEO) and poly(propylene oxide) (PPO) are one example of an amphipathic material with observed thermo-sensitive behavior.[50] The nature of association of the PEO blocks with water and the PPO blocks attempting to shield themselves from water leads to micellation that is affected by different thermal conditions. Natural polymers like proteins and polysaccharides also exhibit thermo-responsive behavior and have been employed in biological research.[15,51]

Of the various thermo-responsive materials, poly(*N*-isopropylacrylamide) (PNIPAm) has attracted some of the most significant attention. PNIPAm demonstrates dramatic thermo-responsiveness in volume around a lower critical solution temperature (LCST), a characteristic of inversely temperature-sensitive polymers. The LCST is the lowest temperature a mixture is miscible for all components. Above this temperature, the mixture becomes partially miscible. Polymers exhibiting LCST behavior are considered inversely temperature sensitive, because polymers generally become increasingly miscible with increases in temperature.[5] The temperature-sensitive swelling behavior is dictated by the hydrophilic-lipophilic balance (HLB);

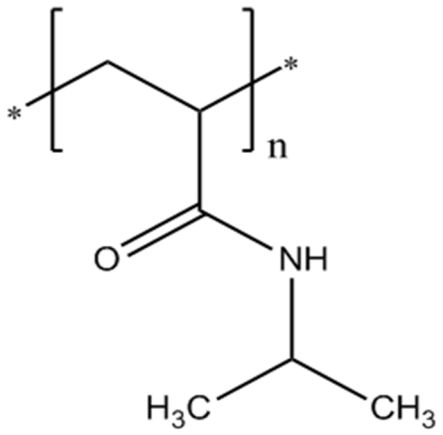

Figure 1.4. Poly (*N*-Isopropylacrylamide) (PNIPAm) repeat unit.

materials obtain optimum HLB at their respective LCST. In the case of PNIPAm (structure shown in Figure 1.4), the hydrophobicity of the amide moieties balance with the hydrophobic isopropyl moieties at the LCST of 33°C.[52] Coincidentally, average body temperature is also approximately 33°C, making PNIPAm a very attractive material in modulated drug delivery systems.[28] At temperatures below the LCST, hydrogen bonds between the amide moieties and water dominate, and the polymer swells. Above the LCST, hydrogen bonding is disrupted by the high energy of the system and hydrophobic interaction increases.[4] These coupled events cause the polymer to collapse leaving an immiscible, globule material.

As in previous examples of coupling pH and analyte-sensitivities, research has also demonstrated the ability to couple pH and thermo-sensitivities in materials containing PNIPAm. To achieve pulsatile drug release, poly(NIPAm-*co*-methacrylic acid) and other pH-sensitive polymers with PNIPAm have been used.[53] Additionally natural polymers such as the abundant,

cationic chitosan have been polymerized with NIPAm to achieve increased loading and control of release kinetics of anionic drugs.[54] These examples of coupled sensitivities utilize interpenetrating networks (IPNs) to combine traditionally incompatible polymers, while retaining responsive properties of each polymer. Mesh size of cross-linked polymers such as those comprising IPNs dictates particle diffusion through the polymer. In hydrated polymers, swelling will increase to an equilibrium swelling value at which the force of swelling pressure is balanced with the force of cross-linking. At this equilibrium swelling state, maximum mesh size is realized leading to maximum diffusion of solute particles. Further efforts in modeling mesh sizes with particle diffusion have been extensively examined.[55,56]

Outside of biological applications, PNIPAm has received attention as draw agents in forward osmosis (FO) processes.[3,57] Traditional FO processes use differences in osmotic pressure between a contaminated water source and a saline solution. Water flows across a semi-permeable membrane from source to the saline solution in order to balance osmotic pressure.[58] The drawback with this method is that the final solution still contains a considerable concentration of salt. Preliminary research has shown that PNIPAm can act alone as a draw agent. The propensity for PNIPAm to swell below its LCST provides the osmotic pressure difference, and up to approximately 75% water recovery is achievable after heating the gel to 80°C. To increase the osmotic pressure difference, poly(sodium-acrylate) (PSA) was cross-linked with PNIPAM, but this results in a dramatic decrease in water recovery from 75% to 22%.[3]

Although PNIPAm exhibits dramatic thermo-sensitive behavior at a biologically relevant temperature, there remains the considerable drawback of slow release kinetics when using this material. As temperature is increased above the LCST resulting in the collapse of the polymer, a thick skin-like layer forms, and water diffusion through this layer is highly retarded.

Additionally, the polymer swelling below the LCST occurs at a very slow rate. These factors combined limit the use of PNIPAm for many applications such as actuators, bio-sensors, and artificial organs.[4] To optimize response kinetics, a porous microstructure and an increased channel network to facilitate rapid convection of water molecules upon response have been theorized as important factors.[4] Using a bicontinuous cubic LLC phase to template nanostructured onto PNIPAm gels have revealed enhancements in both the degree of swelling and the deswelling kinetics compared to unordered PNIPAm gels.[27] This is not only a promising result for enhanced transport and response kinetics, but a method for maintaining mechanical strength of nanostructured polymers as described previously in other templated polymers. This system is able to swell to a great degree and rapidly change its volume when thermally stimulated due to continuous channels in the nanostructure. Mechanical robustness, a necessity in creating viable biological devices or actuators, is improved through the presence of periodic nanostructure throughout the gel.[27] Improvements in the mechanical strength are attributed to the lattice structure exhibited in the templated polymer. When analyzed as a cellular solid, properties like stiffness are extended as much as 1000 times their single value or "cell value." If one period of the bicontinuous cubic phase is considered one cell with a set value of properties, many cells can greatly enhance those properties. The enhancement is realized in the mode of mechanical energy dissipation where energy can either be dissipated as a stretch or bending mechanism, the former being the mechanism of high stiffness materials. Porous hydrogels with an ill-defined lattice are typically dominated by the bending mechanism and buckle under low force. However, nanostructured polymers with highly defined lattice order like those resulting from LLC templating lean more towards the stretch mechanism, consequently, increasing stiffness.[59]

Equilibrium swelling behavior and deswelling kinetics comparing templated and isotropic PNIPAm are shown in Figure 1.5**a** and Figure 1.5**b**, respectively. Here, weight percent water represented the amount of water swelled within the hydrogel and was tested at increasing temperature and time. At room temperature, nanostructure is responsible for an increase in swelling of approximately 400 wt%, and a loss of almost 900 wt% above the LCST at 37°C. In contrast, the isotropic PNIPAm losses roughly just 200 wt% of swelled water across the same temperature range. To test deswelling behavior, each polymer was allowed to reach equilibrium swelling at room temperature and placed in 37°C water for different time periods. Once removed from the water, each polymer was massed, and the weight percent of water remaining was calculated. The effects nanostructure has on deswelling kinetics were substantial as the templated polymer expels close to 750 wt% of its water in just one minute and an additional 90 wt% water after 20 minutes. Conversely, isotropic polymer expelled only 50 wt% of its water and no further de-swelling was observed. An additional noteworthy finding from this research was the lack of

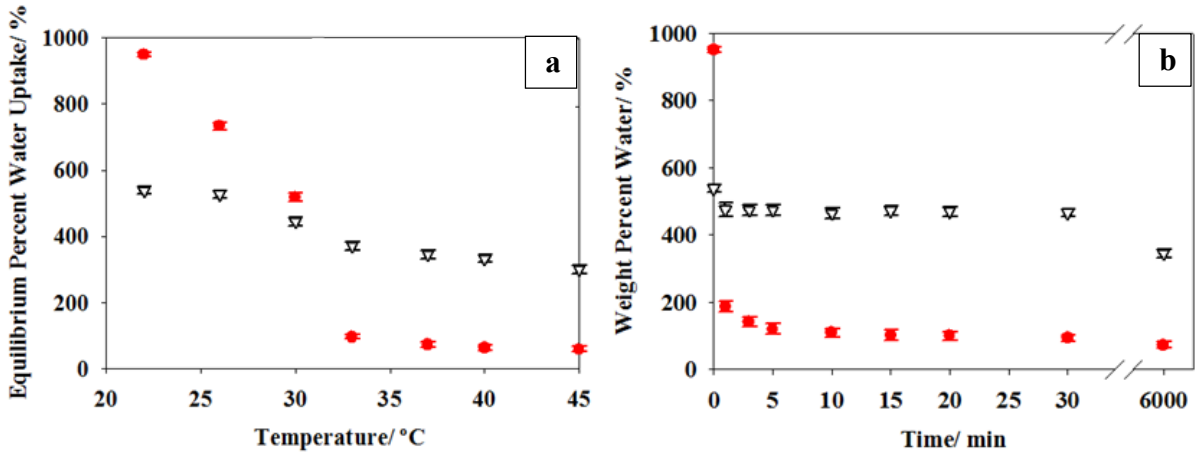

Figure 1.5. Equilibrium swelling behavior and deswelling kinetics comparing templated and isotropic PNIPAm. (**a**) Equilibrium percent water uptake as a function of temperature for isotropic (▽) and bicontinuous cubic LLC templated (●) PNIPAm hydrogels. (**b**) Weight percent water of isotropic (▽) and bicontiuous cubic LLC templated (●) PNIPAm hydrogels as a function of time after transfer from 22 to 37°C water at time zero. Trendlines represent least squares curve fits.[43]

shift in the LCST between templated and isotropic polymer. This drives home the idea that in theory, all LLC templated materials contain an identical chemical structure when compared to unordered polymer. The only difference in the materials is their physical nanostructure; thus, all differences in properties and polymerization kinetics discussed throughout this chapter can be attributed to the templating process.[27]

Additional efforts to improve the hydrated compressive modulus in nanostructured PNIPAm have been examined by introducing the tough, hydrophobic poly(dimethylsiloxane) (PDMS).[26] PNIPAm and PDMS create an interpenetrating network when cross-linked together that exhibited the advantageous properties of individual polymer networks. Thermo-responsive behavior was attributed to PNIPAm, while enhanced toughness was attributed to PDMS. Of particular interest in these studies was the retention of compressive modulus upon dramatic enhancements in water uptake through LLC templating. Figure 1.6 shows compressive modulus as a function of PDMS concentration in both isotropic and templated samples and confirms the

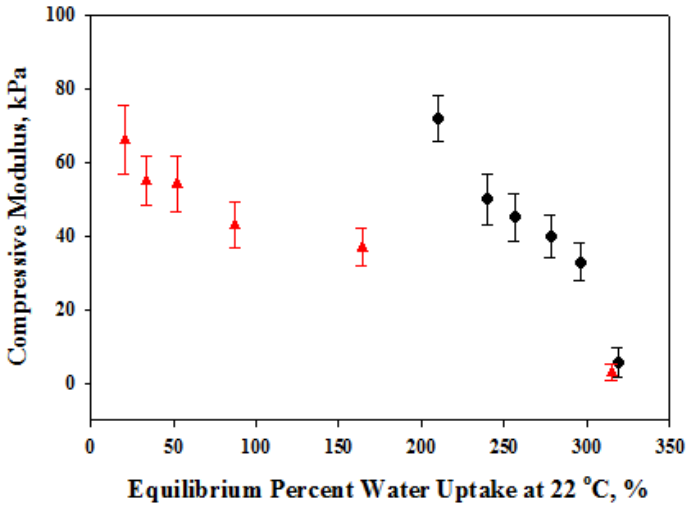

Figure 1.6. Compressive modulus of hexagonal LLC templated (●) and isotropic (▲), PDMS-PNIPAM hydrogels as a function of equilibrium percent water uptake at 22 °C. PDMS concentration represents the total weight percentage of the polymer that is siloxane after surfactant removal and drying. Surfactant was removed prior to analysis.[26]

retention of mechanical integrity in higher water content solely affected by templated LLC order. Therefore, this method provides a promising route for creating materials capable of withstanding application stressors, while simultaneously providing the highly sought stimuli-responsive properties of newer, dynamic materials. The discussed studies employing PNIPAm templated within LLC mesophases exemplify the potential this route may provide in realizing true enhancements in properties of thermo-sensitive polymer materials.

1.3 Summary

Templating of nanostructure onto polymer materials has garnered much interest as outlined above. LLCs provide a very promising method for successful templating with resulting polymers exhibiting controllable properties and kinetics, thereby opening the gate for using such polymers in a broad range of applications. The primary hindrance in accessing the full potential of LLC templating methods for nanostructured polymers lies in the lack of understanding of thermodynamically driven phase separation throughout polymerization. A possible route for addressing this drawback is through detailed characterization of LLC systems for the development of viable thermodynamic models for structural simulations. Interest in nanostructured polymers has also dictated much effort in the area of stimuli-responsive polymer research. Dramatic property enhancements have been observed in the thermo-responsive PNIPAm templated within LLC mesophases when compared to their isotropic counterparts. Research has yet to determine how templating within different LLC mesophases will affect the thermo-responsive behavior of PNIPAm. Hence, this project is motivated by the need for thermodynamic evolutionary knowledge and the potential in templated thermo-responsive PNIPAm in LLC polymer systems.

CHAPTER II. OBJECTIVES

Enhanced transport and mechanical properties realized in nanostructured polymeric materials are of recent interest in many areas including catalysis, biosensors, and drug delivery. The ability to control nanostructure in polymers has become a very promising route for studying enhancements in the transport and response kinetics of these materials. One method that is not only able to transfer nanostructure to polymers, but has shown great promise in the ability to modulate key properties is the templating of polymers within lyotropic liquid crystal (LLC) self-assemblies. Studies have analyzed LLC phase behavior and retention of structure throughout polymerization, however, thermodynamically driven phase separation throughout polymerization continues to impede structure retention in some LLC systems.

LLC templating has also provided new excitement in the area of stimuli-responsive materials that react to chemical or physical stimuli through various mechanisms including dramatic volume changes, thereby swelling or de-swelling a solvent. Studies examining the equilibrium water uptake of a thermo-sensitive material templated with LLC nanostructure exhibited markedly increased ability to uptake water and expel this water when stimulated compared to an unstructured polymer of identical chemical composition. Much room remains for exploring the implications that templated phase and LLC system composition has on stimuli-responsive behavior.

This work is divided into two main sections. The first examines the detailed phase behavior of a basic LLC system to be used as a basis in uncovering key information concerning system thermodynamics. The second section explores LLC templating of a thermo-responsive polymer within different phases to interpret effects phase and system composition have on water uptake and thermo-responsive behavior. Specific objective for this research include to:

1. *Characterize phase morphology and stability by examination of LLC mesophase formed within model LLC polymer systems.*
2. *Investigate the phase behavior and stimuli response of a thermo-responsive LLC templated polymeric material with enhanced transport and response kinetics to determine the relationship between template structure and thermo-responsive behavior.*

Meeting of these objectives will deliver a detailed experimental base for future modeling efforts and key knowledge for controlling properties on LLC templated, thermo-responsive polymers. Characterization of the morphological progression of a simplified LLC system will provide a guide on which to build a thermodynamic model for LLC self-assembly. This model will eventually be used for studying thermodynamic factors leading to phase separation during polymerization and for providing insightful methods for improving the retention of LLC nanostructure within a broader range of possible LLC template systems. Investigation of phase behavior and stimuli response of a thermo-sensitive polymer will afford valuable information concerning the effects of template nanostructure on water uptake and response dynamics. Key trends and observations provided will give new understanding to factors affecting polymer responsive behavior and methods for controlling valuable properties of hydrogels. The outcomes of these objectives will provide further ability to access the evident potential of nanostructured polymeric materials.

CHAPTER III. MATERIALS AND METHODS

3.1 Structural Examination

Achievement of the research objectives required extensive characterization of the LLC templated polymers used throughout the extent of the project. Of great importance and a primary investigation of this work with LLC templated polymer systems was the nanostructure morphology of the parent LLC template prior to polymerization and the resulting morphology of the templated polymer. To analyze nanostructure morphology and structure retention, polarized light microscopy (PLM) and small angle X-ray scattering (SAXS) were employed throughout this research.

PLM provides a simple means to qualitatively determine the morphology of LLC systems by using a series of polarizers to generate an image with features specific to different mesophases. The polarized light microscope is equipped with a polarizer that light passes through before contacting the sample, and an analyzer to create the final image. If a sample is optically anisotropic, two light wave components of differing wavelengths are produced when polarized light passes through the sample. Samples producing two light wave components create birefringence, and the individual waves recombine in the analyzer with interference to create the image contrast.[60]

PLM is limited to observing textures for the hexagonal and lamellar structures. Micellar and bicontinuous cubic structures are optically isotropic, so only one light wave component is produced upon interaction with polarized light producing no image contrast. Hexagonal structures create images with focal conic textures, while lamellar structures produce images containing Maltese crosses.[30] PLM was employed throughout this research prior to polymerization of LLC templated systems to determine the initial mesophase and post

polymerization to qualitatively measure degree of structure retention of hexagonal and lamellar morphologies. Samples were sandwiched between a glass microscope slide and a cover slip. A heating stage equipped to the PLM was used to heat samples above clearing temperatures where the system becomes unordered to promote system homogeneity upon cooling and reassembling of the LLC order.

SAXS was utilized as a quantitative determination of the LLC mesophase in all studies. SAXS is considered the most useful and definitive technique in determining the structure of liquid crystals.[60,61] In SAXS experiments, X-rays are focused on a sample where they can either be absorbed by the sample material, pass through unperturbed, or scatter at an angle (2θ) based upon interactions with the electrons of the sample material. The scattering pattern of these X-rays indicates the position of particular atoms within the sample based upon electron density. This technique is particularly useful for liquid crystals in that the scattering pattern occurs as constructive interference as peaks just like Bragg scattering of crystals due to the periodic structures exhibited by LLCs. These scattering peaks, or Bragg peaks, correspond to the d-spacing of the mesophase lattice; therefore, the peak profile generated by SAXS can be used to directly determine the mesophase of the LLC system and resulting nanostructured polymer. Bragg's law is used to analyze resulting scattering profiles based on d-spacing and is given by Equation 3.1

$$n\lambda = 2d\sin(2\theta) \tag{3.1}$$

where n indicates the scattered peak order, λ is the X-ray wavelength, d is the lattice spacing, and 2θ is the scattering angle relative to the incident X-ray beam.[60] Conventionally, scattering profiles are depicted in terms of the scattering vector, q, which is a measure of distance at the detector. The scattering vector is given by the equation $q = \frac{4\pi}{\lambda}\sin(2\theta)$.

SAXS profiles were generated using an in-house Nonius FR590 apparatus to elucidate LLC mesophase prior to polymerization and structure retention following polymerization. The apparatus used a standard copper target Röntgen tube with a Ni-filtered Cu Kα line of 1.54 Å as the radiation source, a collimation system of the Kratky type, and a PSD 50M position sensitive linear detector.[27]

Stuctural characterization of acrylamide systems templated with the non-ionic surfactants polyoxyethylene (10) cetyl ether (Brij C10) and polyoxyethylene (20) cetyl ether (Brij 58) provided necessary information about morphological tendencies and the ability to tune properties by templating in the variety of LLC mesophases. Chemical structures of Brij C10, Brij 58, and acrylamide are shown in Figure 3.1. Systems in these studies were comprised of acrylamide as monomer, Brij surfactant as LLC, and water as solvent. The concentration of monomer was held constant to mimic previous successful templating of similar systems, while

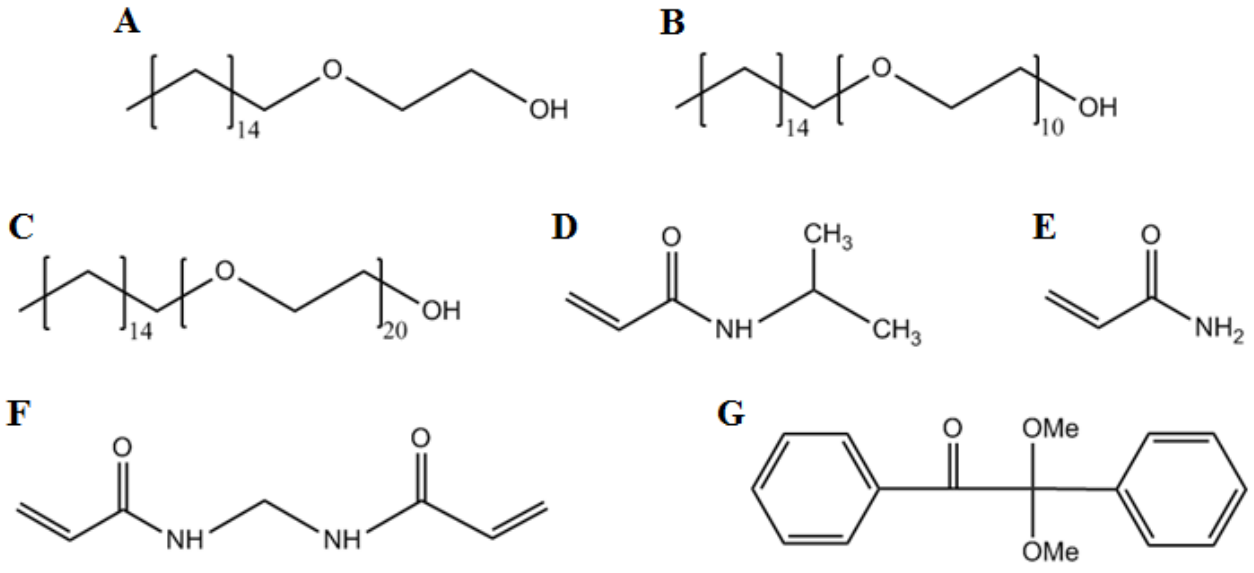

Figure 3.1 Chemical structures of surfactants, monomers, and photo-initiator used in this research. Pictured are **A)** Brij 52, **B)** Brij C10, **C)** Brij 58, **D)** *N*-isopropylacrylamide, **E)** Acrylamide, **F)** *N-N'*-methylenebisacrylamide, and **G)** 2-Dimethoxy-1,2-diphenylethan-1-one (Irgacure-651).

the surfactant concentration was varied to access a variety of LLC mesophases. Surfactant concentrations from 20 wt% to 70 wt% in increments of 5 wt% were studied for both surfactant systems; outside of these limiting concentrations, systems were unordered or phase separated immediately after homogenization. All samples were made with a total mass of 0.5 g and homogenization was achieved through heating and vortex mixing. PLM and SAXS were performed on all samples after a two hour cooling period to allow adequate reassembly of liquid crystalline order.

3.2 Stimuli-Responsive Behavior

Thermally sensitive PNIPAm templated gels were explored to determine direct effects of various LLC systems and their respective template mesophases on equilibrium swelling. These LLC systems were comprised of NIPAm as monomer, *N-N'*methylenebisacrylamide as cross-linker, Brij surfactant as surfactant, dimethoxy-1,2-diphenylethan-1-one (Irgacure 651) as photo-initiator, and water as solvent. Chemical structures of polyoxyethylene (2) cetyl ether (Brij 52), *N-N'*methylenebisacrylamide, Irgacure 651, and NIPAm are shown in Figure 3.1. The three different Brij surfactants were used as templates in this work to analyze the effect of surfactant hydrophobicity on self-assembly and subsequent equilibrium swelling. In Brij 52 systems, cross-linker and monomer concentrations were held constant at 0.5 wt% and 19.5 wt% to mimic literature conditions,[27] while surfactant concentration was increased from 20 wt% to 70 wt% in increments of 5 wt%.

In order to probe effects of cross-linker concentration in addition to surfactant concentration, both parameters were varied independently in Brij C10 and Brij 58 systems. First, surfactant concentration was probed in identical fashion to Brij 52 samples described above.

Cross-linker concentration was then varied between 1, 3, and 5 wt% at selected surfactant concentrations of 20 and 50 wt%. Isotropic controls were made by replacing surfactant with water. All samples were homogenized through heating and vortex mixing.

First, characterization of system morphology in all cases was performed using PLM and SAXS in the same manner as the acrylamide systems described previously. Additionally, morphology was examined following polymerization to examine structure retention. Photo-initiated radial polymerization was achieved using unfiltered ultraviolet light produced by a mercury vapor arc lamp (Omnicure S1500, Lumen Dynamics, Ontario, Canada) at an effective irradiance intensity of 10 $mW \cdot cm^{-2}$ for 20 minutes.

In order to examine equilibrium swelling of the templated hydrogels, samples were polymerized in 5 mL borosilicate vials at the same effective irradiance intensity for a total of 60 minutes. Vials were rotated 90° every 15 minutes to achieve polymerization throughout the entire sample. Three uniform discs were cut from each sample and solvent-exchanged in acetone for 48 hours to remove any unreacted monomer, initiator, and surfactant. Samples were then dried under vacuum for no less than 48 hours.

Equilibrium network swelling studies were performed by allowing each sample to soak in deionized water for 24 hours at each prescribed temperature. At each temperature, samples were removed from water and massed after residual surface water was removed with damp filter paper. This mass along with the mass of the dried sample determined the percent water uptake described in Equation 3.2

$$W = \left(\frac{W_t - W_o}{W_o}\right) \cdot 100\% \tag{3.2}$$

where W is the percent water uptake, W_t is the mass of the water swelled polymer, and W_o is the mass of dried polymer.[27] Network swelling was quantitatively compared to isotropic controls to determine the degree of property enhancement attributed solely to polymer nanostructure.

CHAPTER IV. STRUCTURAL CHARACTERIZATION WITHIN ACRYLAMIDE-BRIJ LYOTROPIC LIQUID CRYSTALLINE SYSTEMS

Polyacrylamide hydrogels templated within lyotropic liquid crystalline mesophases have provided great insight into the ability to control and tune photopolymerization kinetics and significant transport and mechanical properties. Various non-reactive surfactants as well as reactive surfactants have been used to probe these kinetics and properties to discover the benefits of long-range, periodic nano-scale features indicative of LLC mesophase templates.[23,29,32,35,40] Although much is now known concerning structural stability and templating in LLC systems, a void remains in the study of the thermodynamic stability achieved in self-assembly prior to polymerization but lost throughout the duration of polymerization. Modeling techniques that employ key thermodynamic parameters may provide this knowledge and the ability to analyze structural evolution on the molecular level within LLC templated polymer systems. Before viable models and their subsequent use in simulations can be formulated, an in-depth study of a basic LLC system must be performed to aid in baseline modeling efforts.

In this light, the research described in this chapter characterizes the varying morphology exhibited by LLC systems containing acrylamide, Brij surfactant, and water. SAXS and PLM were the primary means of elucidating structure throughout the range of the studied surfactant concentrations. This characterization of LLC morphology showed strong bicontinuous cubic and hexagonal mesophases as well as transitional areas between phases in the two systems studied. This work will be used as a basis for developing thermodynamic models to accurately predict LLC self-assembly and eventually simulate system thermodynamics throughout polymerization.

4.1 Results and Discussion

Acrylamide within non-ionic Brij surfactants was chosen for the model systems due to a number of factors. First, acrylamide is a small, simple molecule that has been shown to associate closely in the hydrophilic domain in LLC mesophases. This is an important factor in reference to modeling efforts with the goal of minimizing interaction parameters in order to simplify models. Modeling efforts and their relation to LLC systems discussed previously in the Introduction chapter were composed of linear block copolymers in water; therefore, minimization of parameters introduced by the addition of closely associating monomer will aid in creating appropriate models in LLC systems. Additionally, acrylamide within the mesophases of Brij C10 and Brij 58 (shown in Figure 3.1) has shown high degrees of LLC order, variability in LLC mesophases, and high degrees of structure retention following photopolymerization, making it an intriguing system to probe structural phase behavior in great detail.

Structural characterization of systems composed of acrylamide, Brij C10, and water self-assembled into a well-defined LLC hexagonal mesophase with observable transitions between bicontinuous cubic and inverse micellar mesophases were confirmed using polarized light microscopy (PLM) and small angle X-ray scattering (SAXS). At concentrations below 30 wt% Brij C10, the sample was free flowing and no birefringent patterns were observed with PLM. Increasing surfactant concentration above 30 wt% resulted in bicontinuous phase behavior as indicated by PLM and SAXS. The transition between the bicontinuous cubic and hexagonal phases was captured at 45 wt% in which the optical texture became apparent due to partial hexagonal phase behavior. Optical textures of the system at 35 wt% (bicontinuous cubic) and 45 wt% (mixed phase) are shown in Figure 4.1**a** and Figure 4.1**b**, respectively. Shown in Figure 4.2**a**, the SAXS profile for 35 wt% depicts a well-ordered bicontinuous cubic phase, while within

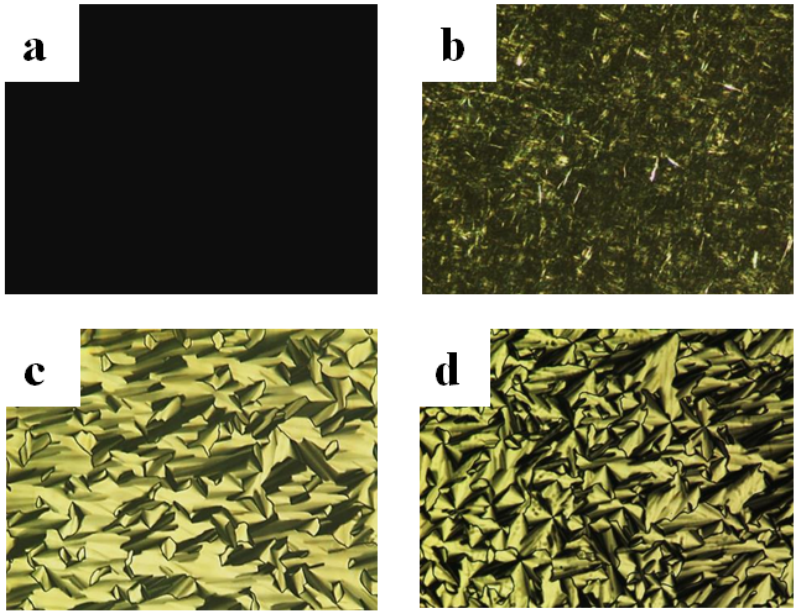

Figure 4.1. Polarized light micrographs of 25 wt% acrylamide within different concentrations of Brij C10 surfactant. Shown are 25 wt% Brij C10 (**a**), 45 wt% Brij C10 (**b**), 55 wt% Brij C10 (**c**), and 65 wt% Brij C10 (**d**).

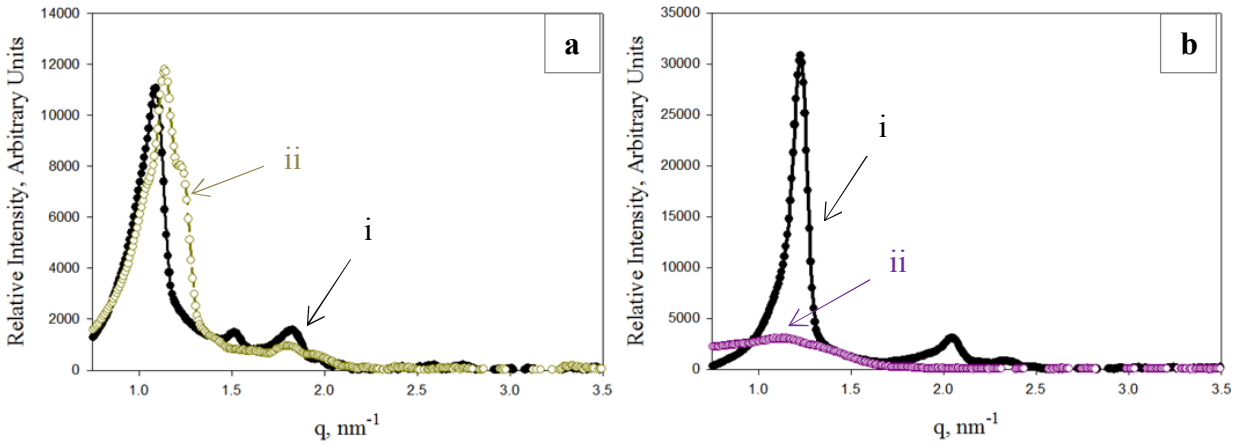

Figure 4.2. Small angle X-ray scattering profiles of acrylamide (25 wt%) and varying concentrations of Brij C10 in water. Shown in (**a**) are profiles of samples containing 35 wt% (i) and 45 wt% (ii). Shown in (**b**) are profiles of samples containing 55 wt% (i) and 70 wt% (ii).

the mixed phase, the profile shows an apparent mixing of LLC structure morphology indicated by a split in the primary scattering peak and variation in secondary peaks, indicating small differences in mesophase lattice spacing.[52] Above the mixed phase transition near 45 wt%, a ell-defined hexagonal phase was accessed at both 55 wt% and 65 wt% Brij C10. The focal conic textures indicative of the hexagonal phase are shown in Figures 4.1**c** and 4.1**d**. Increasing above 65 wt%, the system transitioned to an inverse micellar phase and finally phase separated above 70 wt%. SAXS profiles of the hexagonal at 55 wt% and inverse micellar at 70 wt% phases are shown in Figure 4.2**b**. Here, d-spacing of the SAXS profile (i) matches that of the hexagonal phase, while broad scattering observed in profile (ii) indicates non-ordered inverse micelles.

Structural analysis in the system containing acrylamide, Brij 58, and water exhibited less variation than the Brij C10 system across the studied Brij 58 concentration range. This was attributed directly to a change in the hydrophobicity of the surfactant molecule as Brij 58 has 10 more ethylene oxide units in its hydrophilic domain than Brij C10. The disparity between domain sizes of Brij C10 molecule directed the self-assembly into phases such as hexagonal where the domain sizes are not equal within the system. Conversely, the relatively equal sized domains of the Brij 58 molecule directed self-assembly towards the bicontinuous cubic phase in which hydrophilic and hydrophobic domains exist co-continuously. This was observed in the Brij 58 system as the bicontinuous cubic phase dominated the range of concentrations. Below 23 wt% Brij 58, the system was free flowing with no optical texture observed using PLM. Above 65 wt%, an inverse micellar phase was observed through SAXS. All other concentrations studied formed the bicontinuous cubic phase. Examples of SAXS profiles for the bicontinuous cubic (i) and inverse micellar (ii) phases are shown in Figure 4.3**a**. Although the system was predominately one phase, the strength or order of that phase was shown to fluctuate through

variations in primary peak intensity, peak sharpness, and peak shifting in SAXS profiles. An example of this phenomenon is pictured in Figure 4.3**b** between 25 wt % and 35 wt% where the scattering intensity of the primary peak for 25 wt% is approximately half that of 35 wt%, secondary peaks vary in intensity, and peaks shift between the two samples. Although these differences existed due to different degrees of ordering, d-spacing indicated bicontinuous cubic phase was achieved in both samples.

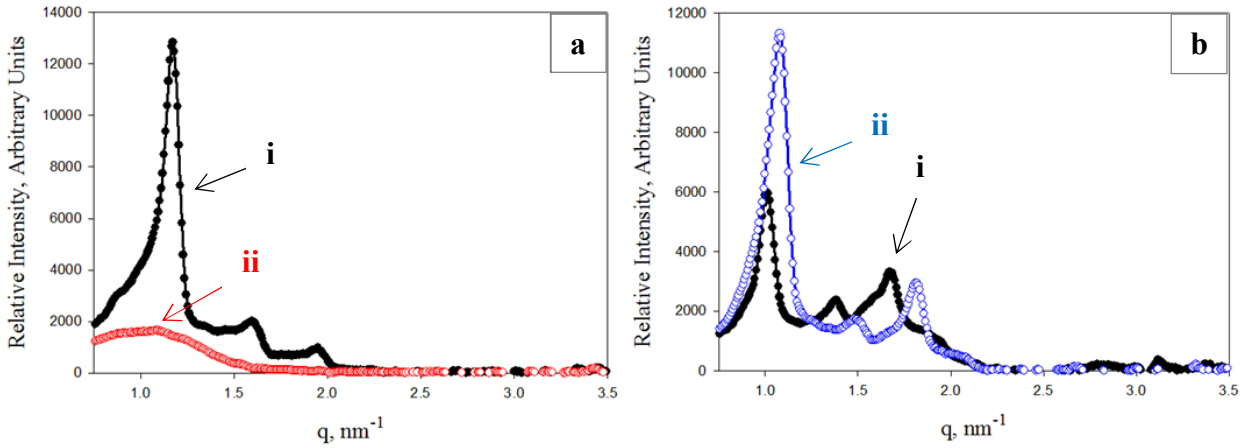

Figure 4.3. Small angle X-ray scattering profiles of acrylamide (25 wt%) and varying concentrations of Brij 58 in water. Shown in (**a**) are profiles of samples containing 55 wt% (**i**) and 65 wt% (**ii**). Shown in (**b**) are profiles of samples containing 25 wt% (**i**) and 35 wt% (**ii**).

4.2 Summary

The structural analysis of these two systems provide the starting point for the modeling necessary for even further control of LLC structure and eventual tuning of polymer properties at the molecular level. Of particular interest are the transitions between mesophases, with concentrations outlined in this research. Here, transitional thermodynamic parameters may

provide essential insight into the thermodynamic destruction of LLC order throughout polymerization currently marring advancement within a variety of LLC templated polymers. The broad ranges of concentrations of surfactant that exhibit the hexagonal phase in the Brij C10 system and bicontinuous cubic phase in the Brij 58 system may also be used to analyze thermodynamic differences in degree of structural order. For instance, the thermodynamic factors and how these factors change around the highest ordered phases may give key information in achieving the strongest LLC mesophases, and how poorly ordered monomer systems might be altered to achieve optimum thermodynamics.

CHAPTER V. WATER UPTAKE AND THERMO-RESPONSIVE BEHAVIOR IN PNIPAM HYDROGELS PHOTOPOLYMERIZED WITHIN LYOTROPIC LIQUID CRYSTALLINE TEMPLATES

Stimuli-sensitive materials have the potential to enhance key properties within a wide range of material applications. Materials in this class exhibit a measurable response upon interaction with physical or chemical cues including molecular adhesion or volume transitions that potentially have the ability to control regulatory processes that mimic similar processes essential to healthy biological pathway function. This responsive behavior has triggered copious amounts of research in utilizing responsive properties to create new materials or significantly enhancing current materials suffering from property deficiencies.[3,5,44,53,54] Stimuli-responsive polymers or "smart gels" have been employed as materials for bio-sensor, actuator, desalination system, and drug delivery vehicle research, but drawbacks for accessing full potential of the responsive mechanism inherent to these smart gels remain.[4,42] Of particular importance in these and many other applications is the kinetics of the gel response. Currently, response kinetics in many studied systems are far too slow to be suitable for use in applications, specifically biological sensing and pathway cascade regulation.

To circumvent the problem of slow response kinetics, photopolymerization within lyotropic liquid crystalline templates has been successfully utilized in creating thermo-responsive hydrogels with enhanced mechanical stiffness and response kinetics. Both properties are dramatically influenced by polymer structure; therefore, LLC templating to induce periodic features at the nanoscale naturally lends itself to stimuli-responsive material research. In fact, one of the most widely researched thermo-sensitive polymers, poly(*N*-isopropylacrylamide) (PNIPAM), has shown great promise in regards to property enhancement through this templating

method.[27] PNIPAm exhibits inverse thermo-responsive behavior in that increasing temperature causes the polymer to become increasingly immiscible in water and become predominately hydrophobic above its lower critical solution temperature (LCST), undergoing a volume transition as the response.

PNIPAm templated with non-ionic Brij 52 surfactant exhibited dramatic increases in response kinetics and degree of equilibrium swelling while maintaining mechanical stiffness compared to a non-templated, isotropic PNIPAm sample as discussed in Section 1.B. The periodicity of templated nanostructure not only provides sufficient avenues for fast water transport into and out of the hydrogel, it also allows for increased mesh stretching and efficient dissipation of mechanical stressors. These factors allow LLC templated PNIPAm to swell to a much greater degree than its isotropic counterpart, while retaining the mechanical strength necessary for many applications. This result was achieved within the bicontinuous cubic phase using Brij 52, but no knowledge of how altering this system morphology through variation of surfactant and surfactant concentration will affect these properties exists.

With these points in mind, this chapter discusses results of equilibrium water uptake studies within three Brij surfactant templates of varying LLC morphology. Different LLC mesophases in each template were determined using SAXS and PLM. The water uptake and thermo-responsive dynamics of templated PNIPAm hydrogels were compared to isotropic PNIPAm to examine the direct effect of templated LLC nanostructure. Of particular interest was the relationship between templating structure and surfactant concentration on the hydrogel behavior. Additional efforts using these systems examined effect of cross-linker concentration on thermo-responsive behavior of PNIPAm hydrogels. Observable trends between strongly

assembling LLC templates and systems exhibiting loosely assembled mixed phases are discussed.

5.1 Results and Discussion

Brij 52 systems containing a constant 19.5 wt% NIPAm and 0.5 wt% cross-linker were studied initially to expand on prior promising results. Analysis of the LLC structure prior to and post photopolymerization utilizing PLM and SAXS revealed peculiar behavior that helps to explain results of hydrogel water uptake and dynamic temperature response behavior. SAXS results shown in Figure 5.1 represent scattering profiles for 50 wt% and 60 wt% Brij 52 before and after polymerization. The scattering peak d-spacing pattern was unrepresentative of any one LLC mesophase before polymerization, yet the d-spacing indicated a lamellar mesophase following polymerization in both samples. Interestingly, when two separate d-spacing indexes were tested on pre-polymerization profiles, the scattering peaks clearly fit for both the hexagonal

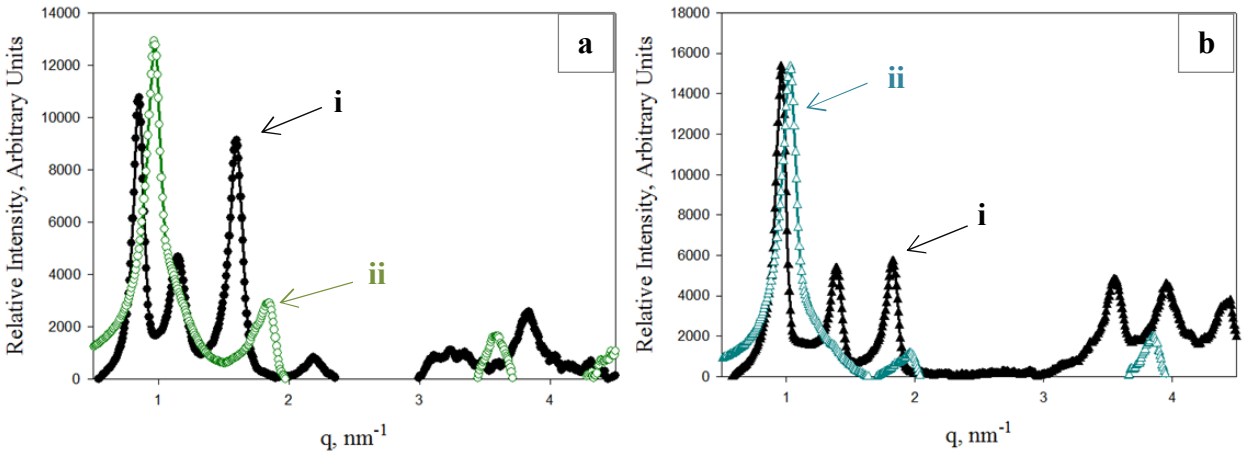

Figure 5.1. Small angle X-ray scattering profiles of 20 wt% monomer (19.5 wt% *N*-isopropylacrylamide, 0.5 wt% *N-N'*-methylenebisacrylamide) and varying concentrations of Brij 52 in water. Shown in (**a**) are profiles of samples containing 50 wt% Brij 52 prior to (**i**) and post (**ii**) photopolymerization. Shown in (**b**) are profiles of samples containing 60 wt% Brij 52 prior to (**i**) and post (**ii**) photopolymerization.

and lamellar mesophases, thus, indicating that a mixed phase of partial hexagonal and lamellar morphology existed in Brij 52 samples across the tested concentration range. The presence of a mixed phase before polymerization was also revealed with PLM as light micrographs indicated optical textures of both hexagonal and lamellar morphologies. Figure 5.2 shows the light micrographs prior to polymerization of 50 wt% (5.2**a**) and 65 wt% (5.2**b**) Brij 52 samples, both

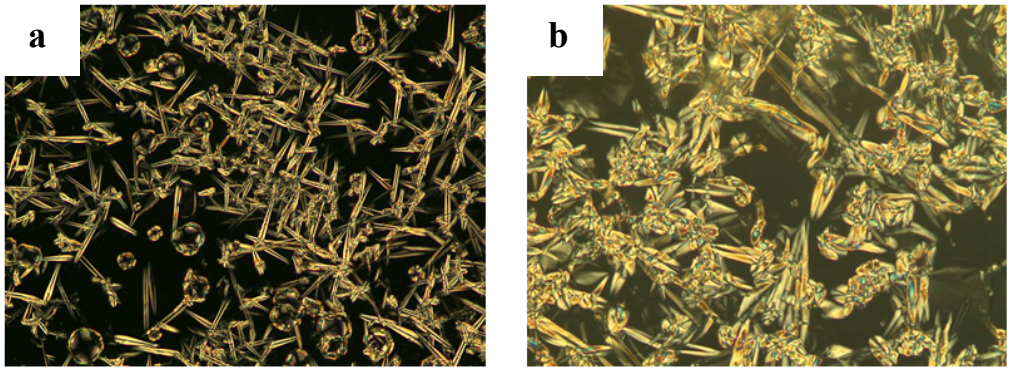

Figure 5.2. Polarized light micrographs of 20 wt% monomer (19.5 wt% *N*-isopropylacrylamide, 0.5 wt% *N-N'*-methylenebisacrylamide) within different concentrations of Brij 52 surfactant. Shown are 50 wt% Brij 52 (**a**), and 55 wt% Brij 52 (**b**).

of which contain focal conic texture of the hexagonal phase and Maltese crosses of the lamellar phase. However, post-polymerization light micrographs did not support existence of the lamellar phase as no optical textures were observed; this may be explained by a decrease in structural domains or domain size associated with the morphological evolution experienced throughout polymerization. For instance, the hexagonal domain structure may no longer be present due to unfavorable thermodynamics leaving unordered PNIPAm domains within surviving lamellar

domains that can be interpreted from powerful, quantitative characterization techniques (SAXS) but not qualitative characterization techniques (PLM).

Equilibrium water uptake in samples containing varying concentrations of surfactant shown in Figure 5.3 revealed interesting trends. At 50 wt%, equilibrium water uptake and water expulsion behavior as temperature increased was comparable to a previous study.[27] Specifically, the templated polymer swelled with approximately 450% more water and expelled more water than the isotropic polymer. Further examination at concentrations above and below 50 wt% revealed no clear trend relating surfactant concentration and corresponding LLC morphology with equilibrium percent water uptake. At 55 and 60 wt% Brij 52, water uptake values at all temperatures except 40°C were comparable and exhibited increased dynamic behavior compared to 50 wt% as room temperature swelling was increased roughly 150%, and water expulsion was

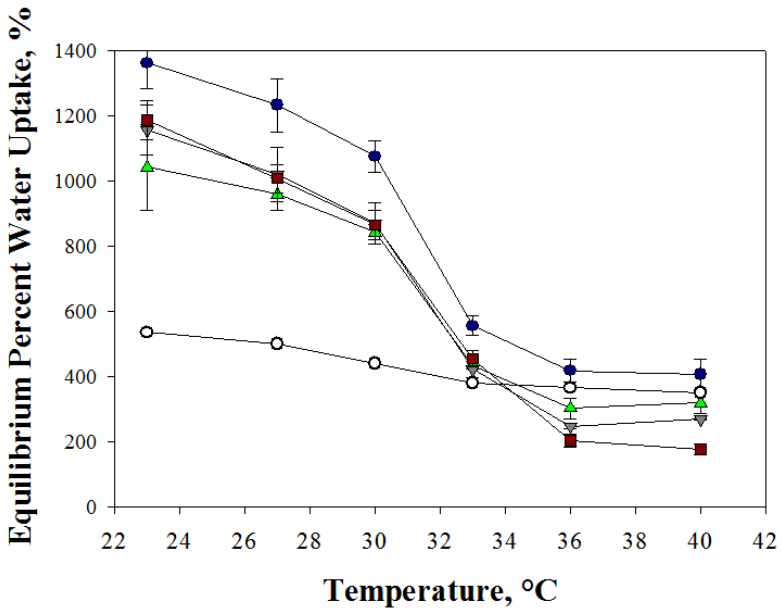

Figure 5.3. Equilibrium percent water uptake as a function of temperature for isotropic (○) and LLC templated with Brij 52 at 45 wt% (●), 50 wt% (▲), 55 wt% (▽), and 60 wt% (■).

increased by a similar amount in the 60 wt% samples. Interestingly, the least amount of surfactant (45 wt%) resulted in an even more significant increase in water uptake reaching up to an 800% increase at room temperature attributed to templated nanostructure. Although 45 wt% samples were capable of swelling to greater degrees, more water became trapped within the hydrogel and did not get expelled above the LCST than all other samples, including isotropic samples. Another aspect elucidated from the swelling behavior in Brij 52 samples was that LCST temperature between all samples remained constant at approximately 33°C even though degree of swelling showed no clear trends with surfactant concentration.

Upon examination of the LLC templated system itself, system behavior and subsequent effects on structure and variability in water uptake may be explained through selection of surfactant and the thermo-sensitive nature of PNIPAm. Brij 52, shown in Figure 3.1, contains only one ethylene oxide unit per molecule with a 16-carbon aliphatic chain. This makes Brij 52 a highly hydrophobic molecule. As described previously, homogenization of each sample was achieved through heating and vortex mixing, a necessity as individual system components exist as solids, and proper mixing would not have been achieved through vortex mixing alone. Upon heating, NIPAm monomer became hydrophobic as hydrogen bonds were broken up between water and the amide constituents, while the hydrophobic, isopropyl constituent effects dominate. This was not an issue at elevated temperatures, but as the system cooled, the transition of NIPAm from a hydrophobic state back to a hydrophilic state in the strongly hydrophobic Brij 52 surfactant caused significant phase separation. The hydrophilic Brij 52 LLC domain occupied a small volume of the overall system compared to the hydrophobic domain, and as NIPAm cooled below its LCST, it was not able to move into this small hydrophilic domain. Phase separation

occurred in this manner across all Brij 52 concentration ranges; therefore, systems could not be polymerized without further intervention.

In order to avoid phase separation induced by NIPAm cooling below its LCST, samples were mixed periodically during the cooling process to keep a homogenous mixture. This process enabled the polymerization of NIPAm templated within Brij 52 mixed LLC mesophases, but may have been a contributing factor, along with the mixed phase nature of these samples, in the lack of correlation between water uptake and surfactant concentration. Without proper ordering of the mesophases throughout the concentration range tested, there was no way to establish understanding of how templating within a particular mesophase affects water uptake. Nevertheless, with the repeatable results of this system, all templated PNIPAm samples were capable of swelling considerable amounts of water compared to isotropic PNIPAm and exhibited dynamic de-swelling of water as temperature approached and surpassed the LCST.

To probe the effects of templating within surfactants of differing hydrophobicity as well as cross-linker concentration, equilibrium water uptake was also examined in PNIPAm systems within Brij C10 and Brij 58. Brij C10 contains a 10-fold increase, while Brij 58 contains a 20-fold increase in hydrophilic ethylene oxide units when compared to Brij 52; therefore, variability in LLC morphology was expected due to hydrophobic effect-driven self-assembly. Changes in cross-linker concentration were made as an exploratory measure within these systems with increases in cross-linker concentration expected to decrease water uptake due to a more tightly bound hydrogel.

To examine LLC template morphology, characterization was performed using PLM and SAXS. The 40-55 wt% Brij C10 range was found to exhibit strong hexagonal LLC order in all samples prior to and post photopolymerization. PLM micrographs of 45, 50, and 55 wt% are

shown in Figure 5.4(**a-f**), all of which contain the focal conic optical texture characteristic of the hexagonal mesophase. Of further note observed in these samples was the lack of connection between optimum thermodynamic phase assembly exhibited at the highest ordered hexagonal phase (50 wt%) and water uptake. The 60 wt% Brij C10 exhibited the same mixed phase-type behavior observed in Brij 52 samples. Optical results of this sample reveal a mixed phase before polymerization (Figure 5.4**g**) and a lamellar phase following polymerization (Figure 5.4**h**). Morphological observations were confirmed with SAXS scattering profiles shown in Figure 5.5**a** obtained post polymerization. At 45 and 60 wt%, d-spacing matched that of the hexagonal and lamellar mesophases, respectively.

Equilibrium water uptake across the concentration range within Brij C10 templates exhibited a clear trend of increasing water uptake with increasing surfactant concentration. The full trend results of water uptake are shown in Figure 5.6. PNIPAm templated in the micellar mesophase shows an increasing water uptake at room temperature of only 100% compared to isotropic PNIPAm. The micellar phase is not considered to contain liquid crystalline order. Surfactant self-assembles into micelles, but there is no long-range order in the position of these micelles. This lack of long range order manifested itself as a small increase in water uptake, yet the increase remained solely attributed to the existence of the LLC template. Templating in the micellar mesophase also produced subtle LCST behavior although the LCST seemed to shift to approximately 30°C. Interestingly, at the higher surfactant concentrations ranging from 40 – 55 wt%, water uptake at room temperature increased with surfactant, while it decreased linearly with increasing temperature, lacking LCST behavior in all samples. Finally, at the highest surfactant concentration (60 wt%), the highest degree of water uptake was obtained as a 475%

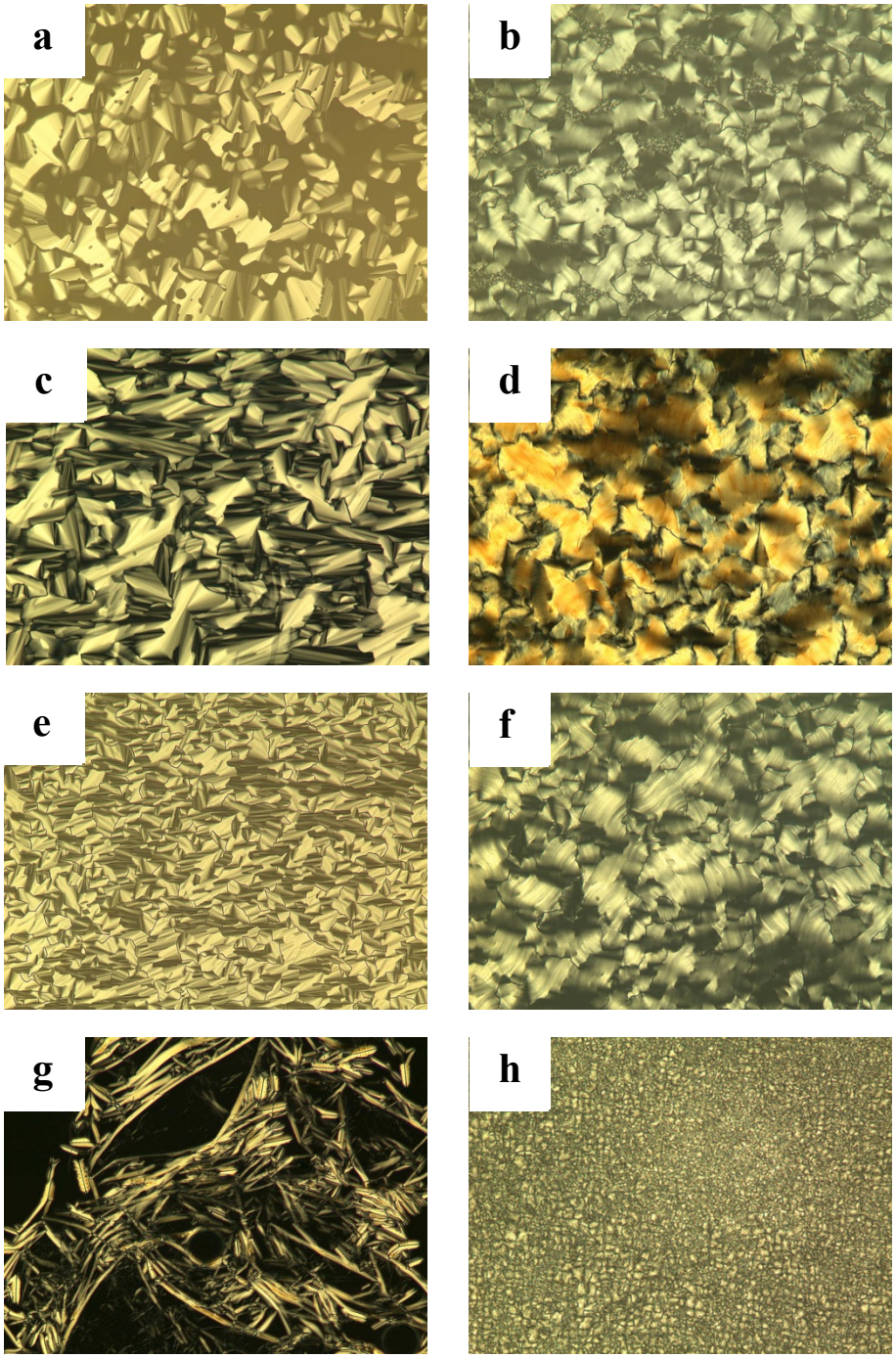

Figure 5.4. Polarized light micrographs of 20.5 wt% monomer (19.5 wt% *N*-isopropylacrylamide, 1.0 wt% *N-N'*-methylenebisacrylamide) within different concentrations of Brij C10 surfactant. Shown are 45 wt% prior to (**a**) and post (**b**), 50 wt% prior to (**c**) and post (**d**), 55 wt% prior to (**e**) and post (**f**), and 60 wt% prior to (**g**) and post (**h**) photopolymerization.

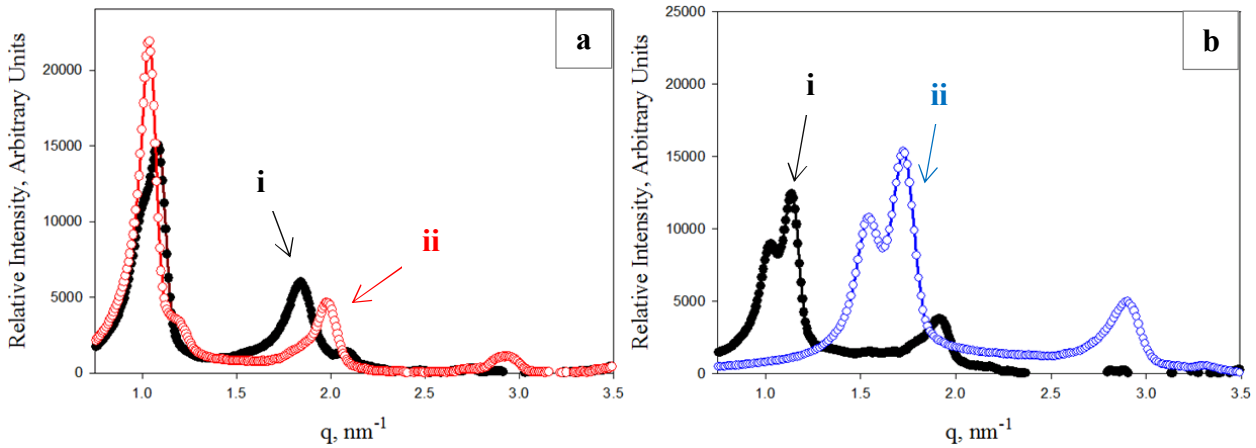

Figure 5.5. Small angle X-ray scattering profiles of 19.5 wt% *N*-isopropylacrylamide and varying concentrations of Brij C10 and cross-linker in water. Shown in (**a**) are profiles of samples containing 1 wt% cross-linker within 45 wt% (**i**) and 60 wt% (**ii**) Brij C10 post photopolymerization. Shown in (**b**) are profiles of samples containing 50 wt% Brij C10 and 1 wt% (**i**) and 3 wt% (**ii**) cross-linker post photopolymerization.

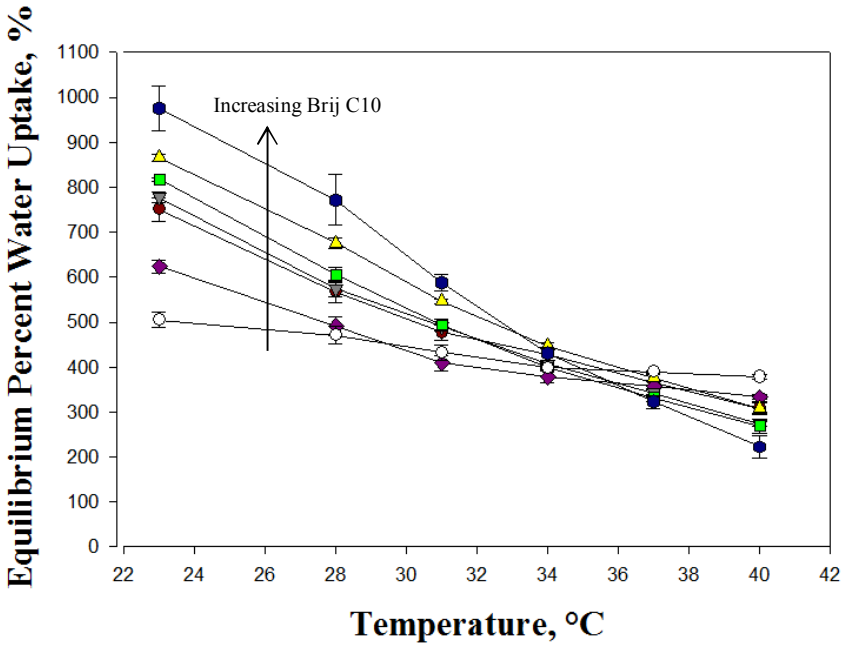

Figure 5.6. Equilibrium percent water uptake as a function of temperature for isotropic (○) and LLC templated with Brij C10 at 20 wt% (◆), 40 wt% (●), 45 wt% (▽), 50 wt% (▷, 55 wt% (▷, and 60 wt% ( )

increase coupled with the dynamic temperature-sensitive behavior observed in Brij 52 samples. It is evident that as LLC templates become increasingly concentrated with surfactant within singular mesophases, resulting hydrogels are able to expand to a high degree influenced primarily by an increase in the nanoscale, periodic features of the respective LLC template mesophase. This concept manifests itself in the trend where increasing surfactant concentration is met with increasing water uptake across most temperatures tested.

These results of templated LLC nanostructure indicated the influence of template ordering and its effect on water uptake across the temperature range of interest. The long-range, unordered quality of the micellar mesophase resembled isotropic sample behavior as micelles polymerized randomly did not produce a porous hydrogel necessary for efficient water transport and swelling. This porous structure was achieved by templating within the hexagonal mesophase, while a linear relationship between water uptake and temperature provided controllable water uptake influenced by water transport through the well-ordered, long-range cylindrical pores. Of particular interest within hexagonal samples was the ability of the structure to withstand volume transitions favored by PNIPAm as temperature increased above its LCST. In fact, these samples did not exhibit LCST behavior influenced by the periodic nature of the templated nanostructure and the efficient stress dissipation throughout the material. As the phase was modulated towards a transitional state above 55 wt%, water uptake continues to increase; thus, surfactant concentration independent of its effect on LLC morphology was strongly connected to water uptake. The mixed phase behavior before polymerization, and the resulting lamellar phase following polymerization similar to studied Brij 52 samples provided the most efficient transport and mesh stretching throughout the PNIPAm hydrogel. Large hydrophilic domains within a loosely cross-linked lamellar phase contributed to these increases in properties.

The study of cross-linker concentration effect on water uptake and temperature-sensitive behavior revealed predictable trends of decreased water uptake with increased cross-linker. Morphology characterization with SAXS and PLM at 50 wt% surfactant shows successful retention of the hexagonal template in Figure 5.5**b** and Figure 5.7, respectively. Because

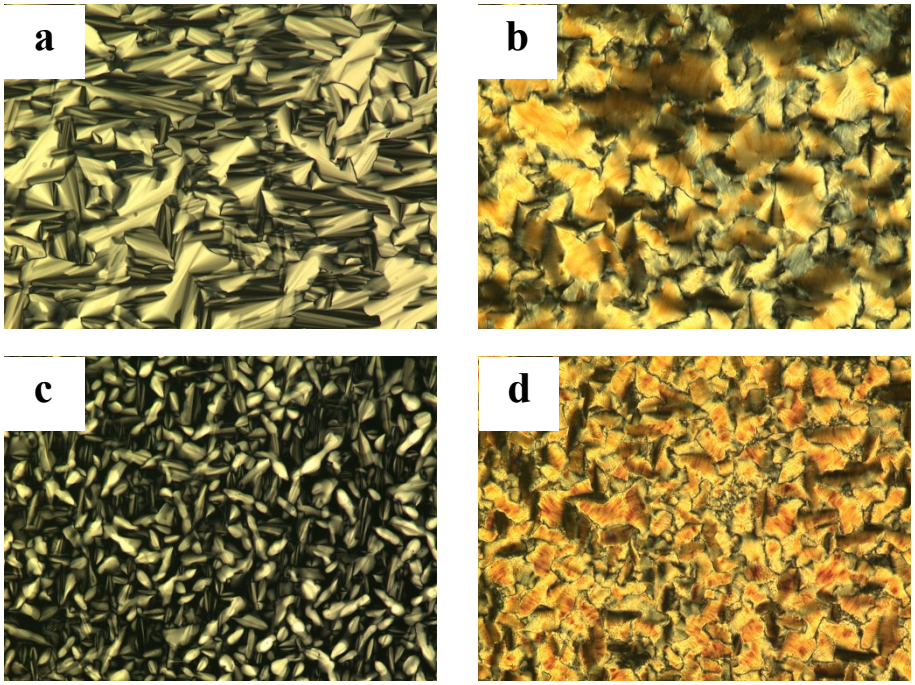

Figure 5.7. Polarized light micrographs of 19.5 wt% *N*-isopropylacrylamide within 50 wt% Brij C10 and different concentrations of cross-linker. Shown are 1 wt% prior to (**a**) and post (**b**) and 3 wt% prior to (**c**) and post (**d**) photopolymerization.

structure remained unchanged, results of water uptake disparity were attributed to a more closely packed hydrogel mesh with increased cross-linker concentration leading to decreases in water uptake. Equilibrium percent water uptake results are shown in Figure 5.8 at 20 wt% (**a**) and 50 wt% (**b**) surfactant. At 20 wt% Brij C10, increasing from 1 to 3 wt% was accompanied by an approximate 250% decrease in room temperature water uptake, and further increasing to 5 wt%

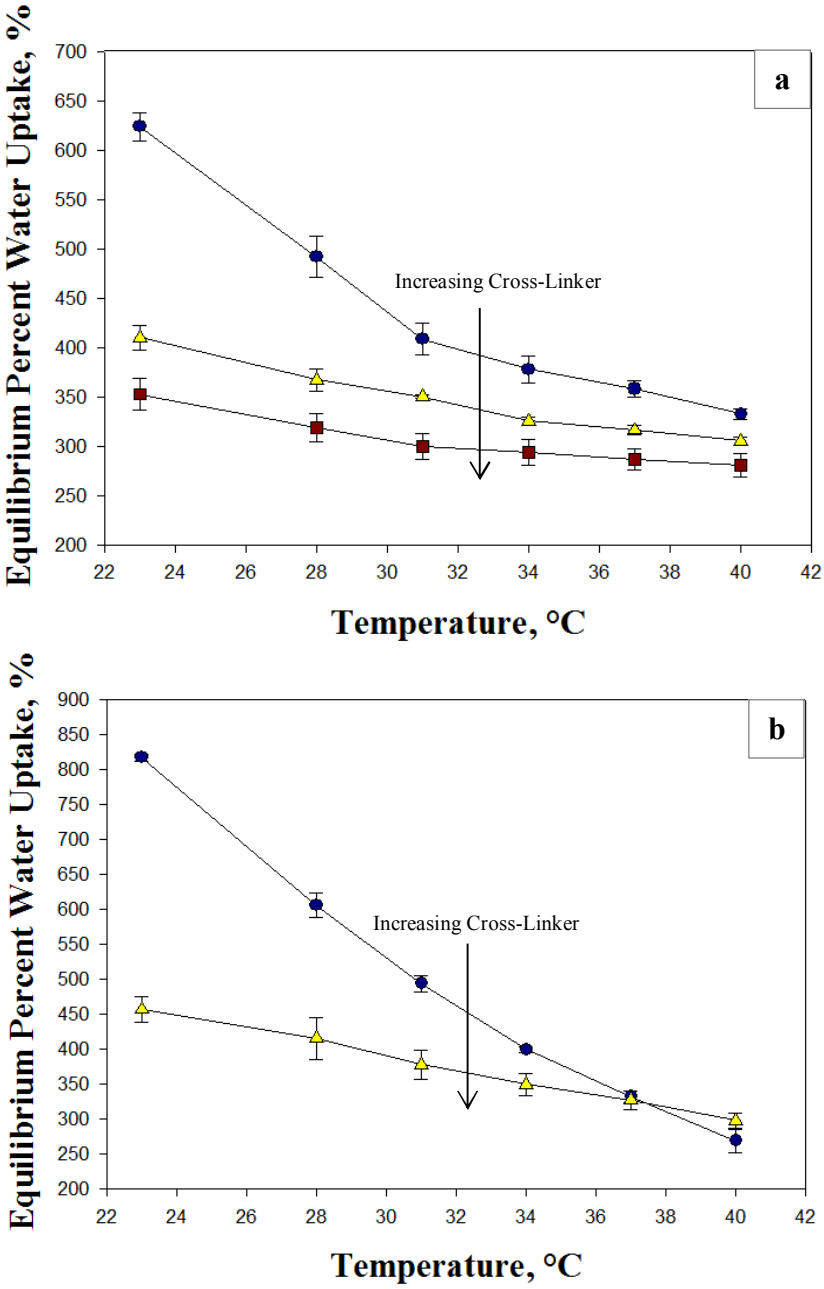

Figure 5.8. Equilibrium percent water uptake as a function of temperature for LLC templated with 20 wt% and 50 wt% Brij C10 with different cross-linker concentrations. Shown in (**a**) are 1 wt% (●), 3 wt% (▲), and 5 wt% (■) cross-linker at 20 wt% Brij C10. Shown in (**b**) are 1 wt% (●) and 3 wt% (▲) cross-linker at 50 wt% Brij C10.

decreased water uptake another 100%. At 50 wt% Brij C10, an even more dramatic decrease in water uptake of approximately 375% was observed by the 2 wt% increase in cross-linker. Five wt% cross-linker at 50 wt% Brij C10 produced brittle polymers that cracked immediately when placed in water. All samples except 1 wt% cross-linker at 20 wt% surfactant exhibited a roughly linear decrease in water uptake with temperature and low cross-linker samples were more dynamic throughout the temperature range. This phenomenon was also observed when comparing between Brij C10 and Brij 52 results; Brij 52 samples showed more water uptake than Brij C10 in all samples at equal surfactant concentration. Cross-linker concentration in Brij C10 had to be increased to get workable hydrogel samples as samples templated with 0.5 wt% cross-linker dissolved during the drying process.

Templating within Brij 58 LLC mesophases produced hydrogels with even less dynamic temperature sensitivity and lower overall water uptake throughout the temperature range. Structural characterization of Brij 58 samples revealed no optical texture in any sample using PLM and d-spacing values indicative of the bicontinuous cubic mesophase using SAXS. Examples of generated SAXS profiles for 50 and 55 wt% Brij 58 are shown in Figure 5.9. As concentration was increased to 55 wt%, scattering peak intensity was greatly increased due to increased liquid crystalline order which correlated to higher water uptake values. Of interest in these results was the supported trend of a closely linear relationship in water uptake with respect to temperature existing in hydrogels templated in a strong LLC mesophase. Meanwhile, mixed phases like those in Brij 52 samples and the high concentration of Brij C10 exhibited less dynamic LCST behavior and overall water uptake. This was partially attributed to changes in cross-linker concentrations needed for testing, but even the bicontinuous cubic phase, having co-

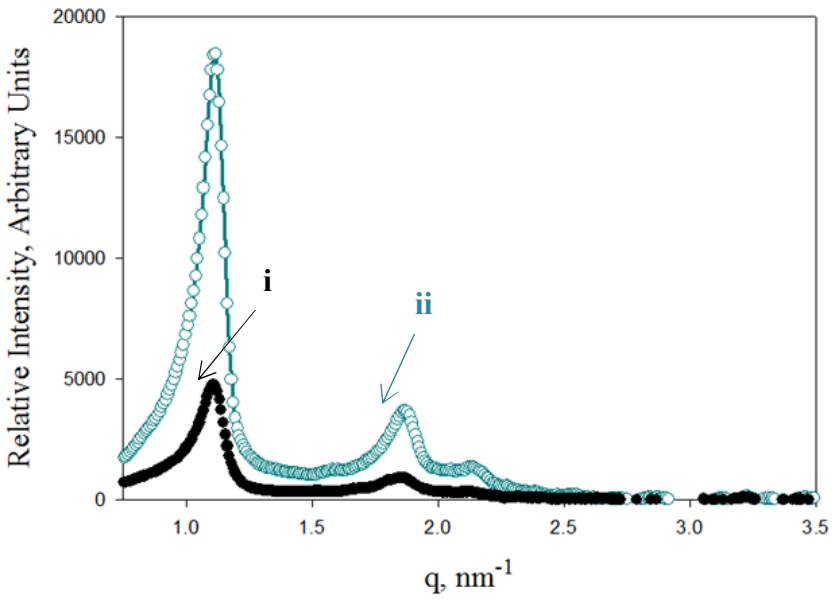

Figure 5.9. Small angle X-ray scattering profiles of 22.5 wt% monomer (19.5 wt% *N*-isopropylacrylamide, 3 wt% *N-N'*-methylenebisacrylamide) within 50 wt% (**i**) and 55 wt% (**ii**) Brij 58 in water post photopolymerization.

continuous intertwined domains optimal for efficient water transport, did not exhibit dynamic LCST behavior.

The decrease in water uptake was highly influenced by testing at 3 wt% cross-linker across the surfactant concentration range to avoid hydrogel disintegration during drying as was the case in Brij C10 samples. Equilibrium water uptake shown in Figure 5.10 exhibits a closely linear dependence of water uptake on temperature throughout the tested concentration range. As was the case for Brij C10 templated PNIPAm, a clear trend existed as water uptake increased with surfactant concentration in Brij 58 templated hydrogels. At the highest templating surfactant concentration (60 wt%), water uptake at room temperature was enhanced by roughly 175% compared to isotropic polymer.

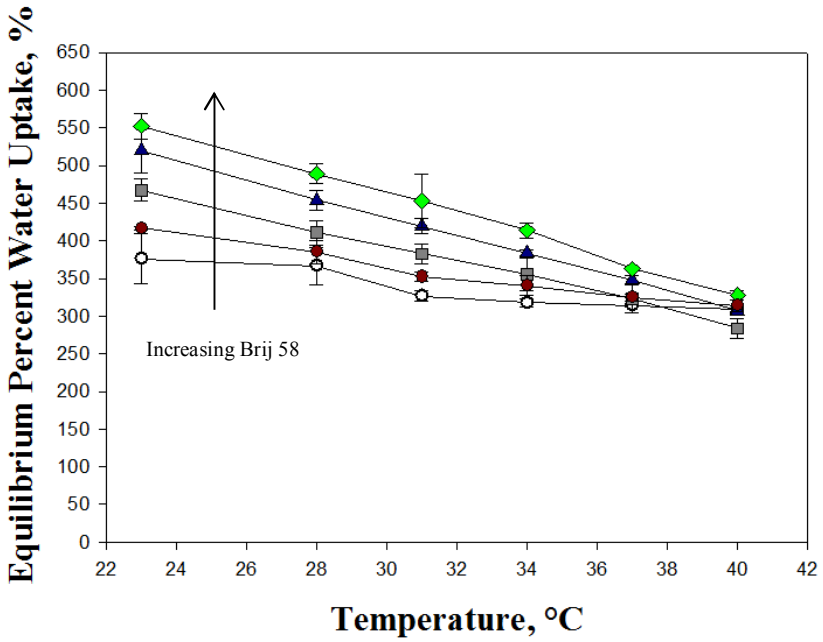

Figure 5.10. Equilibrium percent water uptake as a function of temperature for isotropic (○) and LLC templated with Brij 58 at 20 wt% (●), 50 wt% (■), 55 wt% (▲), and 60 wt% (◆).

Testing the effects of cross-linker concentration was limited to 20 wt% Brij 58 at 3 and 5 wt% cross-linker due to samples disintegrating or becoming too brittle for testing. Results shown in Figure 5.11 indicate expected results with higher cross-linker leading to a decrease in water uptake. Interestingly, the degree of uptake was only decreased by approximately 50% throughout the temperature range and samples templated with 5 wt% cross-linker exhibited more dynamic behavior than any Brij 58-templated sample tested. Similar to samples templated by 20 wt% Brij C10 at 1 wt% cross-linker, the LCST appeared to shift to a lower temperature near 30°C. Although cross-linker concentration could not be held constant across the three tested surfactant concentrations, it is apparent that surfactant and subsequent LLC template morphology plays a key role in water uptake and the nature of PNIPAm thermo-responsive behavior.

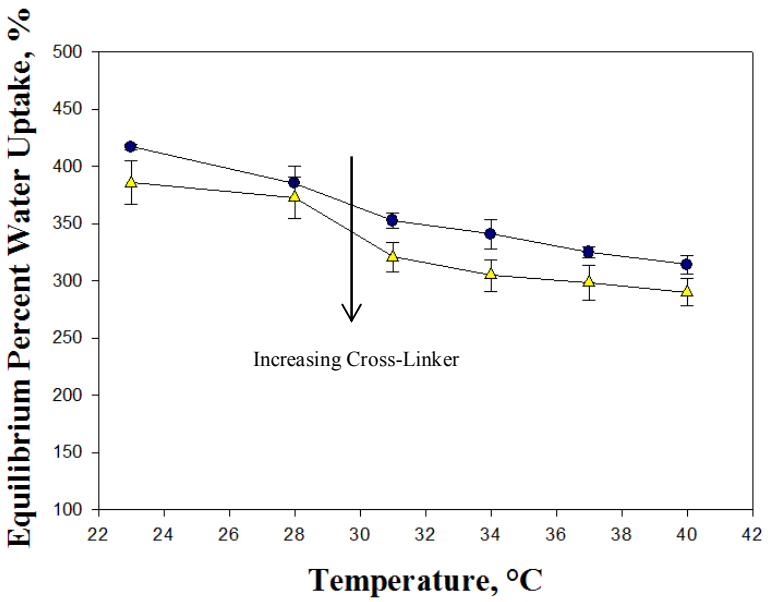

Figure 5.11. Equilibrium percent water uptake as a function of temperature for LLC templated with 20 wt% Brij 58 and cross-linker at 3 wt% (●) and 5 wt% (△).

5.2 Summary

Investigating the effect of templating PNIPAm within various LLC mesophases on equilibrium water uptake and thermo-responsive dynamic behavior in hydrogels revealed a number of interesting results. First, mixed phase behavior exhibited in Brij 52 templated systems leads to dramatic increases in the degree of water uptake at room temperature and a highly dynamic response to temperature increases compared to isotropic hydrogels. There was no clear trend between surfactant concentration and water uptake behavior due to mixed order in self-assembled templates. Replacing Brij 52 with the more hydrophilic Brij C10 and Brij 58 surfactants was accompanied by the appearance of clear trends in which water uptake increased directly with surfactant concentration within the hexagonal and bicontinuous cubic mesophases. These trends were attributed to increasingly dense surfactant templates that were able to transfer

high degrees of periodic order onto hydrogel samples. The periodic nature of the nanoscale features contributes to increased swelling ability as well a means to resist the thermo-responsive collapse in volume characteristic of PNIPAm at elevated temperatures. This feature was shown in the approximately linear decrease in water uptake with increasing temperature for both Brij C10 and Brij 58 samples. Additionally, a tightening of the hydrogel obtained with increases in cross-linker concentration led to a decrease in water uptake across the temperature range of interest.

CHAPTER VI. CONCLUSIONS AND RECOMMENDATIONS

This work has described the detailed structural characterization of a simple lyotropic liquid crystalline/monomer system and structural effects on stimuli-responsive behavior of a polymer templated with lyotropic liquid crystalline (LLC) nanostructure. A model system was selected for detailed structural characterization to provide a basis for thermodynamic modeling efforts necessary for a full understanding of LLC self-assembly and structural evolution throughout photopolymerization within LLC templates. Furthermore, a thermo-responsive polymer was templated within various LLC morphologies to examine the direct effect templated nanostructure has on equilibrium water uptake throughout a temperature range of interest. The previous two chapters described the detailed results obtained over the span of this research. The following chapter will provide a summary of significant research results as well as recommendations for moving this work and future research endeavors in this area forward.

Examination of the structural behavior of acrylamide monomer in non-ionic Brij surfactants provided key information concerning structural progression and transitional areas. In systems containing Brij C10 surfactant, a well-defined LLC hexagonal mesophase with observable transitions between the bicontinuous cubic and the inverse micellar mesophases was observed. Structures were confirmed using polarized light microscopy (PLM) and small angle X-ray scattering (SAXS). The largest ranges of surfactant concentrations self-assembling into one mesophase belonged to 30-45 wt% Brij C10 for bicontinuous cubic and 45-65 wt% Brij C10 for hexagonal.

Upon replacement of Brij C10 with the more hydrophilic Brij 58, less morphological variation was exhibited by the LLC system. The bicontinuous cubic mesophase spanned a surfactant concentration range of 25-60 wt% Brij 58, transitioning to an inverse micellar

mesophase at 65 wt% Brij 58. Below 25 wt% Brij 58, the system did not contain long range order in the micellar phase. The reduced variation in morphology observed in the Brij 58 system was primarily attributed to the difference between surfactant structures. Brij 58 contains ten more ethylene oxide units than Brij C10 making it a much more hydrophilic surfactant. This led to a larger surfactant concentration range of Brij 58 self-assembling into the bicontinuous cubic mesophase containing more evenly distributed hydrophobic and hydrophilic domains.

Investigation of the direct effect of templated LLC nanostructure on equilibrium water uptake within poly(*N*-isopropylacrylamide) (PNIPAm) hydrogels revealed many interesting conclusions. The well-known thermo-sensitive nature of PNIPAm was dramatically affected by templated LLC nanostructure. At room temperature, water uptake was enhanced between 150% to 800% compared to isotropic PNIPAm depending on LLC template morphology. The behavior of water uptake with increasing temperature also revealed curious results that led to the conclusion that the dynamics of the thermo-responsive action of PNIPAm is greatly influenced by the parent LLC template nanostructure. In all studies, the chemical composition between isotropic and LLC templated PNIPAm was identical, therefore, enhancements and differences in the water uptake and thermo-responsiveness of hydrogels was attributed solely to the templated nanostructure.

In water uptake studies using the highly hydrophobic Brij 52 as surfactant, no clear trend was observed between the surfactant concentration dictating LLC template mesophase and water uptake. Regardless, hydrogels templated with Brij 52 underwent the most dramatic enhancements in water uptake at room temperature and also retained the dynamic thermo-responsive behavior indicative of the isotropic hydrogel with a lower critical solution temperature (LCST) of 33°C. All hydrogel samples templated by Brij 52 exhibited peculiar

phase behavior prior to photopolymerization. Before photopolymerization, PLM and SAXS results indicated a mixed phase containing both hexagonal and lamellar domains, whereas upon photopolymerization, the nanostructure shifted to lamellar-like order. Samples templated with 45 wt% surfactant were able to swell approximately 800% more water than isotropic samples at room temperature, but additional water became trapped in the hydrogel at 40°C. The lack of any trend was attributed to an ill-defined structure prior to polymerization.

Probing the effect of templating within different surfactants yielded much more insight into the connection between LLC template morphology and water uptake at varying temperatures. Structural analysis of systems templated with Brij C10 surfactant showed hexagonal morphology for a large range of surfactant concentrations both before and after polymerization while at a high concentration, the system behaved in a fashion similar to Brij 52 systems: a mixed phase before polymerization but a lamellar phase after. Water uptake in these samples was enhanced by as much as 475% compared to isotropic samples, and interestingly, a clear trend of increased water uptake ability with increasing surfactant concentration was observed. This trend was also easily discernible from water uptake results for PNIPAm hydrogels templated with Brij 58. In this case, structural analysis indicated bicontinuous cubic structure before and after polymerization in samples able to uptake high amounts of water compared to isotropic samples.

It is clear that as LLC templates become increasingly concentrated with surfactant within singular mesophases, resulting hydrogels are able to expand to a high degree influenced primarily by an increase in the nanoscale, periodic features of the respective LLC template mesophase. Mixed phase templates are generally unpredictable and are capable of existing with different surfactant species, yet they can produce great enhancements in water uptake attributed

to loosely connected lamellar domains that allow a great degree of hydrogel mesh stretching. This was confirmed with water uptake analysis at increasing cross-linker concentrations. As cross-linker was increased, water uptake decreased in tested samples due to a tighter linked hydrogel mesh as expected.

Remarkably, the dynamic nature of the PNIPAm thermo-response was affected in hexagonal and bicontinuous cubic phases displaying the useful trend information. Instead of displaying inverse LCST behavior with increasing temperature, water uptake decreased linearly with increasing temperature. This is most likely due to the well-defined nature of the templated nanostructure. Although the hexagonal and bicontinuous cubic mesophases provide avenues for adequate water transport, the well-defined structures inherent to each phase provide enough mechanical strength to resist some degree of the force coupled to the propensity of PNIPAm to collapse at increasing temperatures. In samples exhibiting mixed phase behavior prior to polymerization, the resulting hydrogel does not contain the degree of order necessary for resisting this collapsing force. With the knowledge gained in this study, control of water uptake in PNIPAm hydrogels templated in LLC mesophases is possible by simple modulation of surfactant species, surfactant concentration, or cross-linker concentration thereby altering the templated morphology or the periodicity of templated nanostructure.

This research has opened multiple doors for increasing the understanding of thermodynamically driven LLC self-assembly and enhanced stimuli-responsive materials templated within LLC templates. To understand the thermodynamics dictating self-assembly and structural evolution throughout polymerization, modeling efforts must first incorporate the characterization results of acrylamide in Brij surfactants. The experimental characterization can be used as a guide for matching various modeling parameters for not only strongly assembling

morphologies, but also for phase transitional areas that could prove useful in expansion of modeling to real-time radical polymerizations.

Further efforts in developing viable models for accurate simulation of polymerization in LLC templates might explore the effect of adding photo-initiator and characterizing polymerization kinetics through photo-differential scanning calorimetry (pDSC). This experimental characterization will provide information regarding the retention or loss of structure throughout a polymerization by simple analysis of the polymerization rate curve with respect to conversion. With the loss of structure accompanied by a discontinuity in the rate curve, modeling parameters may be built around these events with knowledge of the conversion at which phase separation occurs.

Other alterations to the LLC system might include the use of an anionic surfactant species or a photopolymerizable surfactant. Full phase characterization of these systems can provide a similar basis for development of modeling parameters around different system conditions. Final modeling efforts should incorporate the thermodynamics of the templated polymer to examine structural stability in relation to kinetically stable nanostructured polymers.

Potential routes for expanding the PNIPAm stimuli-responsive study performed in this work are many. First, the kinetics of temperature response of hydrogels templated in the mesophases formed by Brij surfactants must be tested using de-swelling methods. This can be performed by allowing hydrogels to reach equilibrium water uptake amounts at room temperature and placing each sample in water at elevated temperatures for different time periods. Massing of samples after each time period will provide insight into the rate of water expelled induced by temperature changes. The results of de-swelling tests might shed light upon the

changes in response dynamics associated with templating in strong hexagonal and bicontinuous cubic LLC mesophases by revealing altered and controllable kinetics.

Mechanical testing must also be carried out on the studied hydrogels to examine any correlation between polymer toughness and templated nanostructure. Enhanced stimuli-responsive behavior and water uptake must by coupled with the retention of or possible enhancement of mechanical integrity for viable use of these polymers in the variety of proposed new material applications. The mechanism of force dissipation throughout the cross-linked hydrogel may be dramatically affected by templating polymer in different mesophases. If the hydrated material is able to withstand stressors while incorporating stimuli-responsiveness not seen in isotropic hydrogels, templated PNIPAm should be incorporated into various application testing including desalination membranes and drug delivery vehicles.

Finally, alterations to the templating system may allow access of even further controllability of responsive polymers. Using an ionic surfactant or polymerizable surfactant should be examined for possible templating in strong lamellar phases to compare the intriguing results described previously concerning mixed phases transitioning to lamellar phases upon photopolymerization. If templating within a strong lamellar phase results in a continuation of the trends observed in this work, the relationship between loosely connected lamellar domains exhibited by pre-polymerization mixed phases and dynamic temperature response will be strengthened.

Beyond these recommendations concerning the system studied in this work, extension of LLC templating to existing research on broad ranging stimuli-responsive materials should be addressed. For instance, the effect of templated nanostructure on pulsatile drug release materials containing coupled thermo-responsive and pH-responsive polymers might provide unique,

advantageous release kinetics. Enhanced properties realized in LLC templated polymers may also be explored in PNIPAm containing glucose-sensitive units to develop novel diabetes drug delivery. These are just two possibilities within a vast area of materials research that templating of LLC nanostructure has the potential to dramatically influence noteworthy properties like water uptake and thermo-sensitivity studied in PNIPAm throughout this work.

REFERENCES

1. Gin, D. L.; Bara, J. E.; Noble, R. D.; Elliott, B. J. Polymerized lyotropic liquid crystal assemblies for membrane applications. *Macromolecular Rapid Communications* **2008**, *29*, 367-389.

2. Gin, D. L.; Gu, W. Q.; Pindzola, B. A.; Zhou, W. J. Polymerized lyotropic liquid crystal assemblies for materials applications. *Acc. Chem. Res.* **2001**, *34*, 973-980.

3. Li, D.; Zhang, X.; Yao, J.; Simon, G. P.; Wang, H. Stimuli-responsive polymer hydrogels as a new class of draw agent for forward osmosis desalination. *Chemical Communications* **2011**, *47*, 1710-1712.

4. Zhang, X.; Xu, X.; Cheng, S.; Zhuo, R. Strategies to improve the response rate of thermosensitive PNIPAAm hydrogels. *Soft Matter* **2008**, *4*, 385-391.

5. Chaterji, S.; Kwon, I. K.; Park, K. Smart polymeric gels: Redefining the limits of biomedical devices. *Progress in Polymer Science* **2007**, *32*, 1083-1122.

6. Clapper, J. D.; Sievens-Figueroa, L.; Guymon, C. A. Photopolymerization in polymer templating. *Chemistry of Materials* **2008**, *20*, 768-781.

7. Texter, J. Templating hydrogels. *Colloid Polym. Sci.* **2009**, *287*, 313-321.

8. Yan, F.; Texter, J. Polymerization of and in mesophases. *Adv. Colloid Interface Sci.* **2006**, *128*, 27-35.

9. Tsuji, S.; Kawaguchi, H. Colored thin films prepared from hydrogel microspheres. *Langmuir* **2005**, *21*, 8439-8442.

10. Cormack, P. A. G.; Mosbach, K. Molecular imprinting: recent developments and the road ahead. *Reactive & Functional Polymers* **1999**, *41*, 115-124.

11. Sibrian-Vazquez, M.; Spivak, D. A. Enhanced enantioselectivity of molecularly imprinted polymers formulated with novel cross-linking monomers. *Macromolecules* **2003**, *36*, 5105-5113.

12. McKelvey, C. A.; Kaler, E. W.; Zasadzinski, J. A.; Coldren, B.; Jung, H. T. Templating hollow polymeric spheres from catanionic equilibrium vesicles: Synthesis and characterization. *Langmuir* **2000**, *16*, 8285-8290.

13. Morgan, J. D.; Johnson, C. A.; Kaler, E. W. Polymerization of equilibrium vesicles. *Langmuir* **1997**, *13*, 6447-6451.

14. Stevens, M. *Polymer Chemistry: An Introduction;* Oxford University Press: New York, NY, 1999; , pp 551.

15. Dierking, I. Polymer network-stabilized liquid crystals. *Adv Mater* **2000**, *12*, 167-+.

16. Dierking, I.; Kosbar, L. L.; AfzaliArdakani, A.; Lowe, A. C.; Held, G. A. Network morphology of polymer stabilized liquid crystal. *Appl. Phys. Lett.* **1997**, *71*, 2454-2456.

17. Dierking, I.; Kosbar, L. L.; Lowe, A. C.; Held, G. A. Polymer network structure and electro-optic performance of polymer stabilized cholesteric textures - I. The influence of curing temperature. *Liquid Crystals* **1998**, *24*, 387-395.

18. Dierking, I.; Kosbar, L. L.; Lowe, A. C.; Held, G. A. Polymer network structure and electro-optic performance of polymer stabilized cholesteric textures - II. The effect of UV curing conditions. *Liquid Crystals* **1998**, *24*, 397-406.

19. Mizoshita, N.; Kato, T. Liquid-crystal composites composed of photopolymerized self-assembled fibers and aligned smectic molecules. *Advanced Functional Materials* **2006**, *16*, 2218-2224.

20. Lagerwall, J. P. F.; Scalia, G. A new era for liquid crystal research: Applications of liquid crystals in soft matter nano-, bio- and microtechnology. *Current Applied Physics* **2012**, *12*, 1387-1412.

21. Fong, C.; Le, T.; Drummond, C. J. Lyotropic liquid crystal engineering-ordered nanostructured small molecule amphiphile self-assembly materials by design. *Chem. Soc. Rev.* **2012**, *41*, 1297-1322.

22. Antonietti, M.; Caruso, R. A.; Goltner, C. G.; Weissenberger, M. C. Morphology variation of porous polymer gels by polymerization in lyotropic surfactant phases. *Macromolecules* **1999**, *32*, 1383-1389.

23. Clapper, J. D.; Guymon, C. A. Physical behavior of cross-linked PEG hydrogels photopolymerized within nanostructured lyotropic liquid crystalline templates. *Macromolecules* **2007**, *40*, 1101-1107.

24. Zhang, J.; Xie, Z.; She, F. H.; Hoang, M.; Hill, A. J.; Gao, W. M.; Kong, L. X. Nanostructures Generated from Photopolymerization of Poly(ethylene glycol) Diacrylate Templated from Hexagonal Lyotropic Liquid Crystals. *J Appl Polym Sci* **2011**, *120*, 1817-1821.

25. Zhang, J.; Xie, Z.; Hill, A. J.; She, F. H.; Thornton, A. W.; Hoang, M.; Kong, L. X. Structure retention in cross-linked poly(ethylene glycol) diacrylate hydrogel templated from a hexagonal lyotropic liquid crystal by controlling the surface tension. *Soft Matter* **2012**, *8*, 2087-2094.

26. Forney, B.; Guymon, C. A. Improved Stimuli-Response and Mechanical Properties of Nanostructured Poly(*N*-isopropylacrylamide-co-dimethylsiloxane*)* Hydrogels Generated through Photopolymerization in Lyotropic Liquid Crystal Templates. *Soft Matter* **Submitted**.

27. Forney, B. S.; Guymon, C. A. Fast Deswelling Kinetics of Nanostructured Poly(N-isopropylacrylamide) Photopolymerized in a Lyotropic Liquid Crystal Template. *Macromolecular Rapid Communications* **2011***, 32*, 765-769.

28. Schild, H. G. Poly (N-Isopropylacrylamide) - Experiment, Theory and Application. *Progress in Polymer Science* **1992***, 17*, 163-249.

29. Lester, C. L.; Smith, S. M.; Jarrett, W. L.; Guymon, C. A. Effects of monomer organization on the photopolymerization kinetics of acrylamide in lyotropic liquid crystalline phases. *Langmuir* **2003***, 19*, 9466-9472.

30. Forney, B. S.; Guymon, C. A. Nanostructure Evolution during Photopolymerization in Lyotropic Liquid Crystal Templates. *Macromolecules* **2010***, 43*, 8502-8510.

31. DePierro, M. A.; Guymon, C. A. Photoinitiation and monomer segregation behavior in polymerization of lyotropic liquid crystalline systems. *Macromolecules* **2006***, 39*, 617-626.

32. Lester, C. L.; Smith, S. M.; Colson, C. D.; Guymon, C. A. Physical properties of hydrogels synthesized from lyotropic liquid crystalline templates. *Chemistry of Materials* **2003***, 15*, 3376-3384.

33. Lin-Gibson, S.; Jones, R. L.; Washburn, N. R.; Horkay, F. Structure-property relationships of photopolymerizable poly(ethylene glycol) dimethacrylate hydrogels. *Macromolecules* **2005***, 38*, 2897-2902.

34. DePierro, M. A.; Carpenter, K. G.; Guymon, C. A. Influence of polymerization conditions on nanostructure and properties of polyacrylamide hydrogels templated from lyotropic liquid crystals. *Chemistry of Materials* **2006***, 18*, 5609-5617.

35. Clapper, J. D.; Iverson, S. L.; Guymon, C. A. Nanostructured biodegradable polymer networks using lyotropic liquid crystalline templates. *Biomacromolecules* **2007***, 8*, 2104-2111.

36. Odian, G. *Principles of Polymerization;* John Wiley & Sons, Inc.: Hoboken, NJ, 2004; Vol. 4, pp 839.

37. Nagpal, U.; Detcheverry, F. A.; Nealey, P. F.; de Pablo, J. J. Morphologies of Linear Triblock Copolymers from Monte Carlo Simulations. *Macromolecules* **2011***, 44*, 5490-5497.

38. Epps, T. H.; Cochran, E. W.; Hardy, C. M.; Bailey, T. S.; Waletzko, R. S.; Bates, F. S. Network phases in ABC triblock copolymers. *Macromolecules* **2004**, *37*, 7085-7088.

39. Sievens-Figueroa, L.; Guymon, C. A. Polymerization Kinetics and Nanostructure Evolution of Reactive Lyotropic Liquid Crystals with Different Reactive Group Position. *Macromolecules* **2009**, *42*, 9243-9250.

40. Forney, B. S.; Guymon, C. A. Effects of Controlling Polymer Nanostructure using Photopolymerization within Lyotropic Liquid Crystalline Templates. *Chemistry of Materials* **Submitted**.

41. Stuart, M. A. C.; Huck, W. T. S.; Genzer, J.; Mueller, M.; Ober, C.; Stamm, M.; Sukhorukov, G. B.; Szleifer, I.; Tsukruk, V. V.; Urban, M.; Winnik, F.; Zauscher, S.; Luzinov, I.; Minko, S. Emerging applications of stimuli-responsive polymer materials. *Nature Materials* **2010**, *9*, 101-113.

42. Liu, F.; Urban, M. W. Recent advances and challenges in designing stimuli-responsive polymers. *Progress in Polymer Science* **2010**, *35*, 3-23.

43. Ricka, J.; Tanaka, T. Swelling of Ionic Gels - Quantitative Performance of the Donnan Theory. *Macromolecules* **1984**, *17*, 2916-2921.

44. Benns, J. M.; Choi, J. S.; Mahato, R. I.; Park, J. S.; Kim, S. W. pH-sensitive cationic polymer gene delivery vehicle: N-Ac-poly(L-histidine)-graft-poly(L-lysine) comb shaped polymer. *Bioconjug. Chem.* **2000**, *11*, 637-645.

45. De Smedt, S. C.; Demeester, J.; Hennink, W. E. Cationic polymer based gene delivery systems. *Pharm. Res.* **2000**, *17*, 113-126.

46. Chu, L. Y.; Li, Y.; Zhu, J. H.; Wang, H. D.; Liang, Y. J. Control of pore size and permeability of a glucose-responsive gating membrane for insulin delivery. *J. Controlled Release* **2004**, *97*, 43-53.

47. Chu, L. Y.; Liang, Y. J.; Chen, W. M.; Ju, X. J.; Wang, H. D. Preparation of glucose-sensitive microcapsules with a porous membrane and functional gates. *Colloids and Surfaces B-Biointerfaces* **2004**, *37*, 9-14.

48. Cormack, P. A. G.; Mosbach, K. Molecular imprinting: recent developments and the road ahead. *Reactive & Functional Polymers* **1999**, *41*, 115-124.

49. Tanaka, T. Dynamics of Critical Concentration Fluctuations in Gels. *Physical Review a* **1978**, *17*, 763-766.

50. Bromberg, L. E.; Ron, E. S. Temperature-responsive gels and thermogelling polymer matrices for protein and peptide delivery. *Adv. Drug Deliv. Rev.* **1998**, *31*, 197-221.

51. Chen, T. H.; Embree, H. D.; Wu, L. Q.; Payne, G. F. In vitro protein-polysaccharide conjugation: Tyrosinase-catalyzed conjugation of gelatin and chitosan. *Biopolymers* **2002**, *64*, 292-302.

52. Bae, Y. H.; Okano, T.; Kim, S. W. Temperature-Dependence of Swelling of Cross-Linked Poly(n,n'-Alkyl Substituted Acrylamides) in Water. *Journal of Polymer Science Part B-Polymer Physics* **1990**, *28*, 923-936.

53. Brazel, C. S.; Peppas, N. A. Pulsatile local delivery of thrombolytic and antithrombotic agents using poly(N-isopropylacrylamide-co-methacrylic acid) hydrogels. *J. Controlled Release* **1996**, *39*, 57-64.

54. Alvarez-Lorenzo, C.; Concheiro, A.; Dubovik, A. S.; Grinberg, N. V.; Burova, T. V.; Grinberg, V. Y. Temperature-sensitive chitosan-poly(N-isopropylacrylamide) interpenetrated networks with enhanced loading capacity and controlled release properties. *J. Controlled Release* **2005**, *102*, 629-641.

55. Canal, T.; Peppas, N. A. Correlation between Mesh Size and Equilibrium Degree of Swelling of Polymeric Networks. *J. Biomed. Mater. Res.* **1989**, *23*, 1183-1193.

56. Peppas, N. A.; Wright, S. L. Drug diffusion and binding in ionizable interpenetrating networks from poly(vinyl alcohol) and poly(acrylic acid). *European Journal of Pharmaceutics and Biopharmaceutics* **1998**, *46*, 15-29.

57. Li, D.; Zhang, X.; Simon, G. P.; Wang, H. Forward osmosis desalination using polymer hydrogels as a draw agent: Influence of draw agent, feed solution and membrane on process performance. *Water Res.* **2013**, *47*, 209-215.

58. Cath, T. Y.; Childress, A. E.; Elimelech, M. Forward osmosis: Principles, applications, and recent developments. *J. Membr. Sci.* **2006**, *281*, 70-87.

59. Ashby, M. F. The properties of foams and lattices. *Philosophical Transactions of the Royal Society A-Mathematical Physical and Engineering Sciences* **2006**, *364*, 15-30.

60. Collings, P.; Hird, M. *Introduction to Liquid Crystals Chemistry and Physics;* The Liquid Crystals Book Series; Taylor & Francis Inc.: Bristol, PA, 1997; , pp 298.

61. Fried, J. *Polymer Science and Technology;* Prentice-Hall, Inc.: Upper Saddle River, NJ, 2003; Vol. 2, pp 582.